2017

Interactions of Polymers and Energetic Materials

Rebecca M. Levine
University of Rhode Island, rlevine@chm.uri.edu

INTERACTIONS OF POLYMERS AND ENERGETIC MATERIALS

BY

REBECCA M. LEVINE

A THESIS SUBMITTED IN PARTIAL FULFILLMENT OF THE

REQUIREMENTS FOR THE DEGREE OF

MASTER

OF

SCIENCE

IN CHEMISTRY

UNIVERSITY OF RHODE ISLAND
2017

MASTER OF SCIENCE
IN CHEMISTRY

THESIS

OF

REBECCA M. LEVINE

APPROVED:

Thesis Committee:

Major Professor Jimmie Oxley

Co-Major Professor James Smith

Brenton DeBoef

Otto Gregory

Nasser H. Zawia
DEAN OF THE GRADUATE SCHOOL

UNIVERSITY OF RHODE ISLAND
2017

ABSTRACT

Trace explosive detection is the primary way for quick and easy sampling of various surfaces in a check-point environment, e.g. an airport. The swabs used for commercial explosive detectors, such as ion mobility spectrometers, are made of various materials. The difficulty in collection and analysis of explosive traces is that the swabs must be effective at adsorbing as well as desorbing materials, i.e. pickup from the surface and release into the detection device. This dichotomy results in a tradeoff for development of new swabs. Generally, desorption is considered to be the more desirable property; therefore, Teflon is one choice for commercial swabs. It would be ideal to develop a swab with both enhanced adsorption and desorption. One way to accomplish this is to apply an electrostatic charge to commercial swabs. This enhances their attraction to explosive particles, but once the swab is placed in the inlet of commercial detection instrument, the charge is dissipated, and desorption of the particles into the instrument proceeds as usual.

Methods of generating electrostatically charge swabs was determined; triboelectric charging vs corona charging was compared examining magnitude of the charge, reproducibility and stability, and effects of humidity. The magnitude of charge necessary for enhanced collection of particles was evaluated using an electrostatic voltmeter to measure charge and various means to measure particle pickup. Corona charging was determined to be more effective. Enhancement of collection was judged by comparing results of corona charging swabs to those achieved by contact swabbing. Two variables were examined: the analyte and the substrate from which the analyte is removed. The swab material was Nomex. In each case but three, collection of an

analyte by an electrostatically enhanced swab outperformed the traditional contact swabbing. Evaluation was determined by a rigorous quantification by mass spectrometry of the analyte picked up by the swab and the analyte remaining on the substrate after swabbing. When analytical protocol was not amenable to a particular analyte or substrate a commercial explosive trace detection instrument was used. It was found that the substrate morphology played a bigger role in pickup of analyte than the particular analyte.

In order to eliminate biological warfare agents, both heat and halides are used. Ideally, these agents would be destroyed without dispersing them. The approach to create a polymeric-sprayable matrix would allow dispersion of an iodine-producing pyrotechnic, without dispersing the biological weapon, and when initiated would produce both heat and iodine gas. This matrix will provide iodine vapor and a long-lasting flame, not an explosion, to control dispersion of the threat.

A two-part foam was formulated based on polyurethane chemistry, i.e. a diisocyanate combined with polyol to produce a urethane linkage. Each component of the foam (e.g. isocyanate, polyol, catalyst, blowing agent, surfactant) was experimentally adjusted to achieve the best foam based on expansion, structural integrity, and cell uniformity. Since the polyol is the most adjustable component in the foam, an investigation of commercial and synthesized energetic polyols was performed. The structures of the energetic polyols were verified by LC-MS and FTIR and characterized for heat flow by DSC. Once the structures of the energetic polyols had been proven, it was formulated into a polyurethane foam which was characterized for heat of decomposition, by SDT, for heat of combustion by bomb calorimetry, and

structurally by FTIR. Documenting heat flow with SDT helped to determine that the structural modification increased heat release and lowered ignition temperature compared to the standard polyurethane foam. The formulated polyurethane foam was then tested for expansion against increased solids loading. When optimal solids loading was determined (>70%), the pyrotechnic foam was ignited in a bomb calorimeter. The heat released and iodine production was quantified.

ACKNOWLEDGMENTS

Thank you to my advisors Dr. Jimmie Oxley and Dr. James Smith for accepting me into their research group and giving me the opportunity to be exposed to some great unique research. To the funding agencies: Department of Homeland Security (DHS) and Defense Threat Reduction Agency (DTRA) for funding this research. To my entire research group (past and present) sharing lab space with me and for their help with various projects. A particular thank you to Austin Brown for being my guide in the lab and always there with a helping hand. In addition, Dr. Matt Porter for his assistance with the DTRA project. I would especially like to thank Dr. Joe Brady for mentoring me through some real interesting science and your boisterous laugh always kept me going through hard times.

To my family for encouraging me through graduate school even when things were tough and supporting my decisions. To my closest friends, Jaclyn Herbst, Ashli Simone, Laura Hendrickson-Rabin, and Julie Whelan for your countless hours of listening to my struggles and always loving me and being there for me. I couldn't ask for better friends. To my fiancé, Dr. Matt Mullen, we have grown together through some of the best times and worst times during graduate school. Thank you for always supporting me and recognizing my potential as a chemist. I don't think I would have made it through this without you. I love you with all my heart and I can't wait to spend the rest of my life with you. Lastly, a special thanks to my wonderful animals: Penny Lane, Bunsen, and Jasmine. Your unconditional love has helped me through this journey more than your little fluffy minds will ever comprehend.

PREFACE

This thesis is prepared in the manuscript format. Chapter 1 is titled Electrostatically-enhanced swabbing for near field sampling; this work was funded by DHS. Chapter 2, Potential Biocides: Polymer Packaging of Iodine containing Pyrotechnics was funded by DTRA through grant HDTRA1-14-0027 and part of the manuscript is in preparation for publication. This document is written in Manuscript Format. Guidelines for formatting have been followed here and in the entirety of this document.

TABLE OF CONTENTS

LIST OF TABLES

LIST OF FIGURES

Figure Page

Manuscript 1

Electrostatically Enhanced Swabbing for Near-Field Sampling

By Rebecca Levine, Jimmie C. Oxley, James L. Smith, Devon Swanson, Alex Yeudakimau, and Victoria Stubbs

Chemistry Department

University of Rhode Island

140 Flagg Road, Kingston, RI 02881

Submitted as confidential government report

ABSTRACT

Explosive detection often depends on collection of particles by swabbing potentially contaminated surfaces. We have found that the pickup of particles by commercials swabs can be improved by applying an electrostatic charge to the swab. Two methods of generating electrostatically charged swabs were tested-- triboelectric versus corona discharge. They were compared examining charge magnitude, reproducibility, stability, and effects of humidity. The charge necessary for collection of particles was evaluated using an electrostatic voltmeter and measuring particle pickup. Enhancement of collection was judged by comparing pickup by electrostatically enhanced Nomex® swabs with that achieved by contact swabbing. The efficiency of contact versus non-contact electrostatic swabbing was tested against two variables—analyte (TNT, RDX, PETN, and ammonium nitrate) and 13 substrates. Mass spectrometry was used to quantify analyte pickup by mass balance of the analyte on the swab and remaining on the substrate. When quantification by mass spectrometry was impossible, electrostatic swabbing was evaluated and compared to contact with an explosive trace detector (i.e. ion mobility spectrometer).

INTRODUCTION

Effective explosive detection is of critical importance to law enforcement and government agencies. The Department of Homeland Security (DHS) has defined instruments which can pass certain tests, i.e. detecting specified explosives in a set amount of time, as explosive detection systems (EDS) or explosive trace detectors (ETD). A "trace explosive" is defined as not visible to the human eye, generally, material at the nanogram level [1-2]. Collecting trace amounts of explosive and transitioning them to a detector is the weak link in detection protocol. Much research in explosive detection is aimed at the development of selective and sensitive detectors, but these gains can be offset by inefficient analyte collection and introduction. Current swabs use materials, such as paper, Nomex, or Teflon, to mechanically scrape the analyte from a surface [3]. A dichotomy in explosive trace detection is that swabs must be effective at sorption as well as de-sorption, i.e. sorption to the surface and release into the detection device.

Generally, de-sorption is considered to be the more desirable property; therefore, polytetrafluoroethylene (PTFE) known as Teflon,™ is one choice for commercial swabs [2]. Traditionally, swabbing is by direct contact. The contact swabbing of hands, headdresses, and medical appliances can increase the amount of contaminants on the swab and can be personally invasive. The ideal swabs would both enhanced sorption and de-sorption and require no contact with the subject or object.

This study considers application of electrostatic charge to commercial swabs. This can be accomplished three ways: triboelectric charging (friction), induction charging, or conduction. The classic conductive charging method uses a Van de Graaf

generator. The head of the Van de Graaf generator is negatively charged, and when a neutral object comes into contact with it, the charge is transferred [4]. This method was initially examined, but the charge was non-directional and short-lived on surfaces. Thus, only triboelectric and corona charging were further investigated.

When two materials with different electron affinities come in close proximity, the transfer of electrons creates separation of charge between the two surfaces [5-10]. The static charge created on the two surfaces can be positive or negative, depending on their relative position in the triboelectric series [7]. The triboelectric series lists materials in order of their preference to obtain a charge of relative magnitude in relationship to other materials (Figure 1.1).

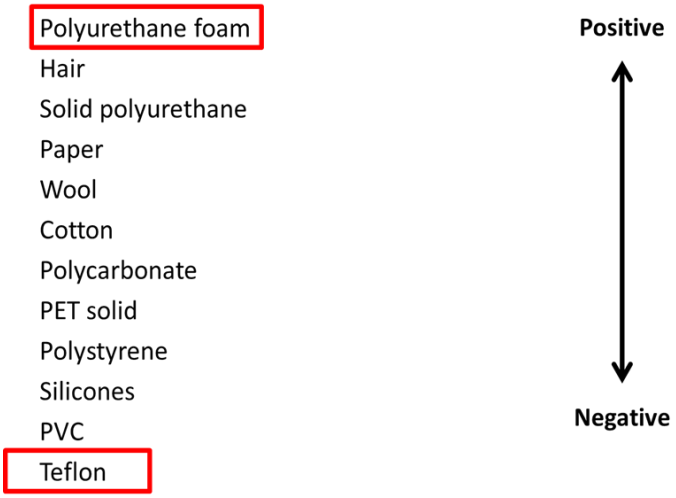

Figure 1.1. The Triboelectric Series

The further away two materials exist on the triboelectric series, the higher the resulting magnitude of charge on the two materials. For example, PTFE is highly negative on the triboelectric series, and friction between it and a highly positive material in the series should result in two oppositely charged materials [5-6, 9]. This method of charging is termed "triboelectric charging." This method might also result in transfer of contaminants. Inductively charging a swab can be achieved without

contact. A corona needle (pinner) attached to a high voltage supply with low current ionizes the surrounding air molecules. When the pinner is in close proximity to a grounding plate, electrons migrate toward the grounding plate, passing through intervening surfaces, in this case, a swab. Thus, the swab is charged. The grounding plate may play a role in increasing the uniformity of charge (a concept investigated in this study). Inductive charging is used commercially, in one application to create a permanently polarized material, termed an electret. Electrets, like the Swiffer®, are formed by exposing a material to polarized electric fields at high temperature [11-14].

In theory, any material with a measurable relative permittivity should be subject to electrostatic enhancement [15-16]. In this work, the potential for non-contact electrostatic swabbing was investigated and benchmarked to performance of standard contact swabs.

EXPERIMENTAL METHODS

Swabs & Substrates

Teflon (PTFE) and Nomex swabs were supplied by FLIR Detection. PTFE-coated fiberglass and cotton swabs were supplied by DSA Detection and no modifications were made. Substrates were cut from bulk material to approximately 1/2 inch by 2 inch. Bytac® substrate, (fluoroethylene propylene with vinyl backing) was purchased from Saint-Gobain. Aluminum foil substrate (the dull side) was obtained from Berkley Jensen. PTFE and cotton substrates were obtained from pieces of FLIR and DSA Detection swabs, respectively. Vinyl, high density polyethylene (HDPE), and polycarbonate substrates were purchased from McMaster-Carr. (The latter two required a scroll saw to cut). Ballistic nylon was purchased online from Amazon. The

ABS (acrylonitrile butadiene styrene) substrate was printed into flat pieces on a MakerBot 3-D printer. The white Nylon 1000 substrate was purchased from Rockywoods (The white substrate was used because the solvent extracted the black dye). Zipper substrates were plastic pull tabs (polyurethane) purchased from Ohio Travel Bag. The cardboard substrate was created by pulling apart a cardboard corrugated sheet so that just the first layer was used. Polypropylene wrapping material, verified by FTIR using attenuated total reflectance (ATR) was also used.

Scanning Electron Microscopy (SEM)

Scanning electron micrographs were obtained at 20 kV in secondary ion mode on a JEOL 5900 SEM of some of the substrates and swabs. Secondary ion mode was used because it specifically focused on the surface morphology.

Analytes

Initially, commercial sugar and sodium chloride were used as surrogates for organic explosives and inorganic energetics, respectively. These were sieved to control particle size to approximately 800 microns. Organic explosives 2,4,6-trinitrotoluene (TNT), 1,3,5-trinitro-1 3 5-triazacyclohexane (RDX), Pentaerythritol tetranitrate (PETN), C-4, and an inorganic energetic material ammonium nitrate (AN) were obtained from military or industrial sources (Figure 1.2).

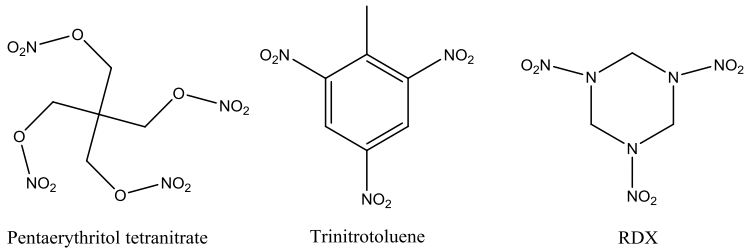

Figure 1.2. Chemical structures of PETN, TNT, RDX

Humidity Measurements

A humidity chamber was built using a humidistat and glove box. Controlled humidity environments were achieved with saturated salt solutions [17]. Experiments at 0% humidity used dry compressed air.

Dry Transfer

Trace quantities of solid analyte were placed on surfaces as solutions of known concentrations via micro-syringe and solvent allowed to evaporate. This resulted in an unrealistic distribution of analyte on the surface (e.g. coffee rings); therefore, a dry transfer method was developed [18]. The solution of analyte was placed by Eppendorf pipette (2-20 μL) onto a strip of Bytac®. The solvent was allowed to evaporate from the Bytac, and the resulting residue on the Bytac® was transferred to the desired substrate by rubbing the Bytac over the substrate in one direction.

Preparation of Analytes

Analytical standards were made by starting with a 1 mg/mL solution of the analyte and performing subsequent serial dilution in appropriate solvents. For organic explosives, the solvent was either HLPC grade acetone or 50:50 HPLC grade acetonitrile: Optima® water. For inorganic explosives the solvent was ultra-pure 18 MΩ water. Each test series began by directly spiking 500 ng of analyte onto Bytac. Subsequent analysis of the amount of analyte remaining on the Bytac, the substrate, or the swab was performed as follows. For the organic analytes, the substrates were put in 15 mL polypropylene conical vials with 7-10 mL of HPLC grade methanol. In addition, each substrate without analyte went through the same extraction conditions as controls. Vials were shaken for ~1 min, vortexed for ~1 min, sonicated for 15 min,

vortexed ~ 1 min, and transferred to clean glass conical vials. Vials were evaporated to dryness using an Organomation Nitrogen evaporation system with compressed air and a water bath at 40°C. Solutions were reconstituted with the appropriate amount of 50:50 acetonitrile: water to achieve a final concentration of 500 ng/mL. The solution (400 µL) was transferred into a LC vial, syringe filtered through a PTFE 0.22 µm filter, and 20 µL of a 5000 µg/mL solution of 2,4-dichlorophenoxyacetic acid was added to each vial as an internal standard.

Quantification of Organic Analytes

For organic analytes, quantification was accomplished by an Accela 1250 liquid chromatograph with Thermo Scientific TSQ Quantiva triple quadrupole mass spectrometer (LC/MS). A heated electrospray ionization (HESI) source created ions that went to an ion transfer tube at 300°C. Conditions used in HESI analysis Table 1.1.

Table 1.1. Conditions for HESI source of mass spec (V=voltage & AU= arbitrary unit)

Conditions for HESI source	
negative ion spray voltage (V)	2500
sheath gas (AU)	40
auxillary gas (AU)	12
sweep gas (AU)	1
vaporizer temperature (°C)	260

Sample injections of 20 µL were by a CTC Analytics HTS PAL auto sampler from glass LC sample vials with PTFE septa. The 20 µl aliquot was at a flow rate of 300 µL/min with initial conditions of 95 % aqueous 200 µM ammonium chloride, 200 µM ammonium acetate, 1% formic acid and 5% methanol, then at 5 min the conditions changed to 5% aqueous 200 µM ammonium chloride, 200 µM ammonium acetate, 1% formic acid and 95% methanol. At 7 minutes the solvent ratio returned to the initial conditions and held until the completion of injection cycle at 8 minutes. The

LC column was a Thermo Scientific Acclaim Polar Advantage II C18 (PA2, 2.1x50 mm, 3 µm, 120 Å). Multiple reaction monitoring (MRM) transitions are shown for each compound in Table 1.2.

Table 1.2. MRM transitions for organic explosive analytes

Compound	Precursor (m/z)	Product (m/z)	Collision Energy (V)	Retention Time (min)
PETN	351.03	46.15	16.93	5.6
	351.03	62.11	10.25	
TNT	226.03	46.24	26.58	5.0
	226.03	165.93	15.31	
	226.03	196.09	12.83	
RDX	257.12	35.24	32.50	4.8
	257.12	46.01	28.35	
	257.12	82.17	10.25	
2,4-Dichlorophenoxy acetic acid	219.00	89.04	34.88	6.4
	219.00	125.00	27.04	
	219.00	160.94	13.03	

Curves were analyzed and linearly correlated between the ratio of internal standard and the analyte which was weighted ($1/x^2$) by Thermo Xcalibur Quan Browser software version 3.0.63. An example of a standard curve can be seen in Figure 1.3. Dynamic range for PETN analysis was from 10 to 2500 ng/mL; for TNT, 25 to 5000 ng/mL; and for RDX, from 10 to 2500 ng/mL.

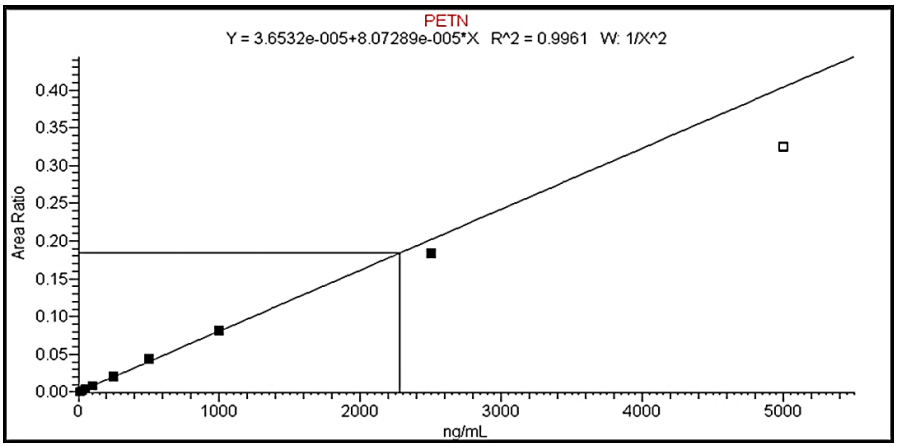

Figure 1.3. Example of a calibration curve for PETN

Explosive Trace Detectors (ETD)

The commercial ETD used in these experiments was a Morpho Itemiser DX ion mobility spectrometer (IMS). The compatible swab for this instrument was PTFE-coated fiberglass. The sensitivity of the ETD was evaluated by dosing swabs directly with 10-250 nanograms of PETN or 100-10,000 nanograms AN. For PETN 100 ng of analyte was deposited from a solution of acetone onto Bytac® and allowed to dry. For AN 500 ng of analyte was deposited from a solution of water onto Bytac and allowed to dry. For both analytes, the dry transfer method was employed from Bytac® to various substrates (Figure 1.4). For contact swabs, the swab physically contacted the substrate with ~7 N of force. Electrostatic swabs were charged at -20 kV, 2 inches from the swab for 5 seconds. Voltages were recorded with a 3M 718 electrostatic voltmeter, and passed along the substrate from a distance of ~10 mm. In each test, after swabbing the substrate, the swab was placed in the heated inlet of the IMS. If an IMS response of "NO ALARM" occurred, the swab was recharged and the substrate re-swabbed; this attempt to get an alarm was repeated up to three times.

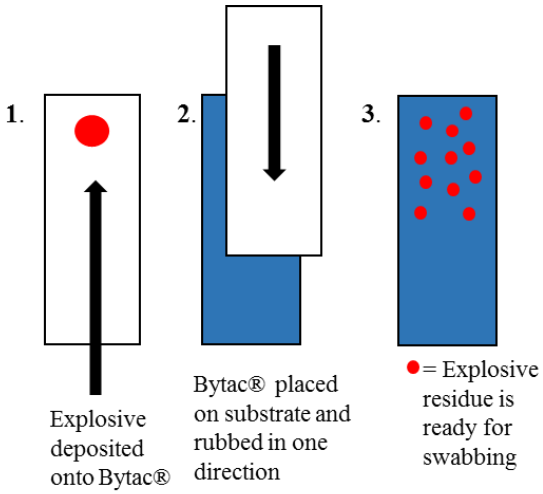

Figure 1.4. Setup for the dry transfer of analyte to each substrate

RESULTS AND DISCUSSION

Bulk Measurements

As a proof of concept, electrostatic pick up of visible amounts of surrogate analytes, sucrose and sodium chloride, was performed (Figure 1.5, Table 1.3). An electrostatic charge was applied to PTFE swabs by rubbing the swab on a polyurethane foam roller. This triboelectric charging method resulted in swabs with charges ranging from -1.32 kV to -3.61 kV. For the sucrose and sodium chloride data, the relative humidity (RH) was 41% and 24%, respectively. On an index card, 100 milligrams of analyte was placed, and the charged swab was held over it at a fixed distance—0, 10, 20, 30, 50, and 100 millimeters. For comparison, an uncharged swab, was tested in a similar fashion. Efficiency of pickup was judged by the amount of analyte remaining on the index card. Each test was done in triplicate. The nature of the analyte, organic versus ionic, did not appear to affect the extent of pickup. However, as expected, the farther away the swab was from the analyte, the less efficient the pickup. There was a significant drop off from 20 mm to 30 mm. Results suggest the maximum effective distance for any analyte transfer to a triboelectrically charged swab is likely to be ~50 mm. Without a charge no significant amount of mass was picked up at a distance greater than 0 millimeters. (Table 1.4).

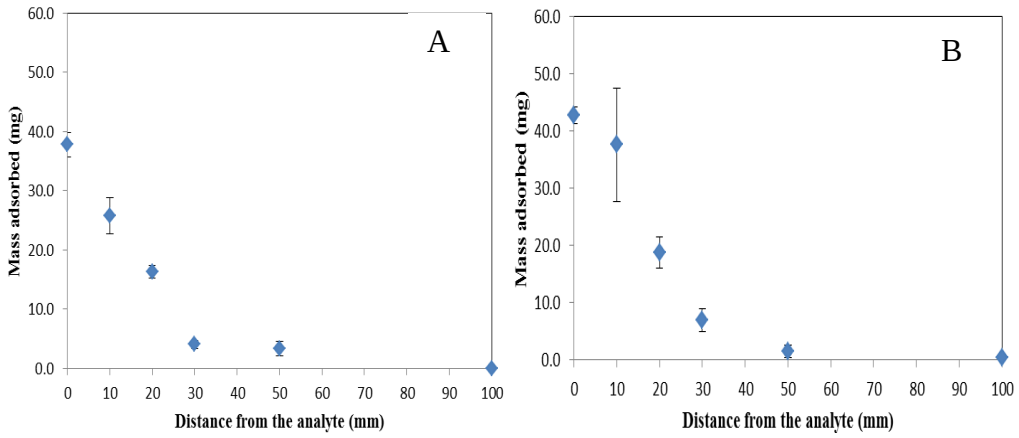

Figure 1.5. Decrease of sucrose (A) and sodium chloride (B) pickup as a function of distance

To determine the minimum charge necessary for pickup of analyte, 30 mg of either PETN or AN were placed on an index card, and a PTFE swab was triboelectrically charged, to voltages ranging 0.1 kV-1 kV. From a height of 10 mm, analyte pickup was attempted. Both the index card and swab were weighed on an analytical balance. Both analytes were picked up, even at these low voltages, although, the highest pickup was (5 mg) which amounts to ~15% recovery (Figure 1.6).

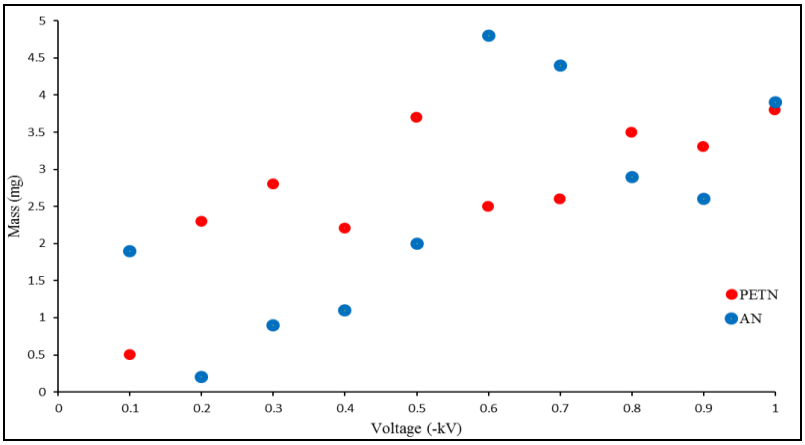

Figure 1.6. Pickup of PETN and AN at low voltages in milligrams

Table 1.3. Bulk Measurements of mass pickup of sucrose & NaCl on charged swabs

Distance (mm)	Mass sucrose adsorbed (mg)	Charge (-kV)	Average sucrose absorbed (mg)	Std Dev (mg)	Distance (mm)	Mass NaCl adsorbed (mg)	Charge (-kV)	Average NaCl absorbed (mg)	Std Dev (mg)
0	39.8	2.85	**37.8**	2.0	0	41.1	2.31	**42.7**	1.4
0	38.5	3.14			0	42.5	2.64		
0	35.0	2.47			0	44.5	3.18		
10	27.3	2.85	**25.8**	3.0	10	51.4	3.61	**37.6**	9.9
10	21.6	2.41			10	32.3	1.81		
10	28.6	3.34			10	29.0	2.67		
20	14.9	2.17	**16.4**	1.1	20	17.6	2.25	**18.7**	2.7
20	17.4	2.85			20	22.5	2.52		
20	16.8	1.32			20	16.1	2.01		
30	3.5	2.75	**4**	0.7	30	9.4	3.47	**6.9**	2.0
30	3.6	2.35			30	4.6	2.64		
30	5	2.91			30	6.8	2.83		
50	3	2.34	**3**	1	50	2.5	3.00	**1.5**	1.1
50	5	2.72			50	2	3.59		
50	2	1.89			50	0	2.73		
100	0	3.12	**0**	0	100	0	2.25	**0.4**	0.2
100	0	2.46			100	1	3.28		
100	0	2.38			100	0	3.50		

Table 1.4. Bulk measurements pickup of sucrose and NaCl on uncharged swabs

Distance (mm)	Mass sucrose adsorbed (mg)	Charge (kV)	Distance (mm)	Mass NaCl adsorbed (mg)	Charge (kV)
0	1.5	0.02	0	1.9	0.03
0	1.1	0.08	0	2.8	0.02
0	0.5	0	0	3.1	0.05
10	0	0.03	10	0	0.04
10	0	0.08	10	0.2	0.07
10	0.4	0.05	10	0.3	0.01

SEM Micrographs

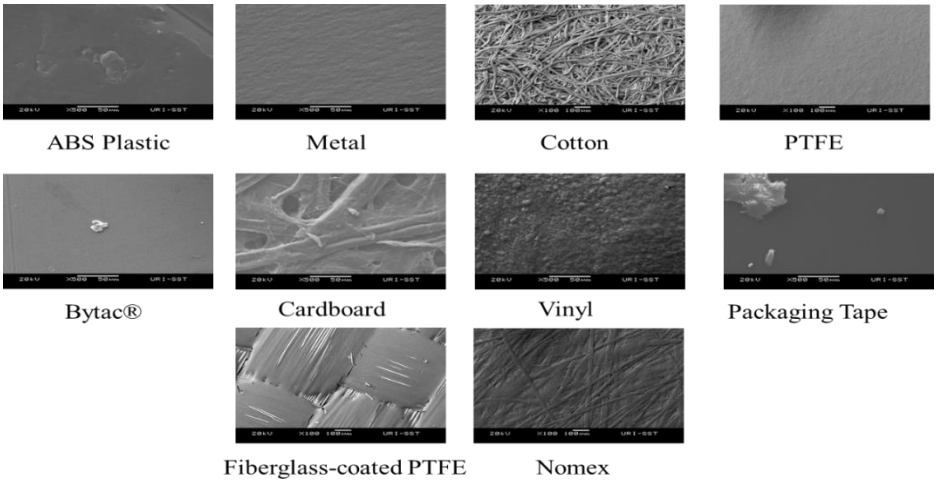

Figure 1.7. SEM micrographs of select substrates (top rows) and swabs (bottom row)

Method for charging swabs

To charge swabs inductively, a pinner was fixed over an unheated hot plate base which had been covered with a perforated metal (zinc coated steel) grounding plate (Figure 1.8). The grounding plate had a screw in one corner and a wire which was fixed to the screw of a traditional electrical outlet (A schematic is shown in Figure 1.9). The contact was tested with a multi-meter to verify proper grounding. Since the use of inductive charging relies on the attraction of a charge through the swab to a base, various bases were examined (Table 1.5). Tests were performed charging at -20 kV and 2 inches from the swab for 5 seconds at 40% RH. Voltages were measured using a 3M 718 electrostatic voltmeter, and a static dissipater was used to eliminate excess charge before each experiment. Results, shown in Table 1.5, indicated no change in the base surface would be necessary.

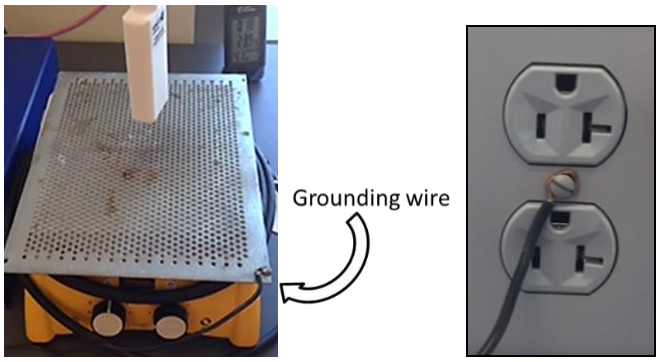

Figure 1.8. Hot plate with grounding wire and the grounding connection at outlet

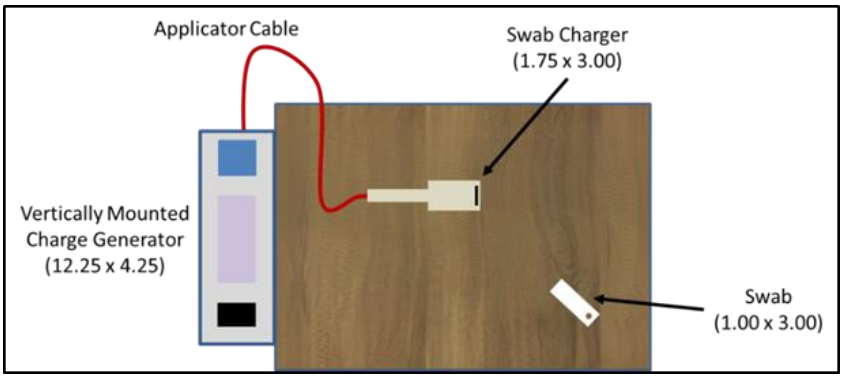

Figure 1.9. Schematic of the inductive charger

Table 1.5. Potential Surface for Charging Station tested with PTFE and Nomex swabs

Nomex swab, base (thickness in)		Initial Charge (kV)	wait time 30 sec (kV)	wait time 60 sec (kV)	Teflon swab, base (thickness in)		Initial Charge (kV)	wait time 30 sec (kV)	wait time 60 sec (kV)
Hotplate 1.504	1	-11.98	-12.21	-12.31	**Hotplate** 1.504	1	-9.34	-6.34	-5.17
	2	-13.03	-13.87	-12.21		2	-8.53	-6.22	-5.03
	3	-13.04	-13.42	-11.98		3	-7.53	-5.40	-4.98
ABS 0.132	1	-1.12	-1.22	-1.13	**ABS** 0.132	1	-0.64	-0.57	-0.57
	2	-0.97	-0.97	-0.97		2	-1.51	-1.49	-1.39
	3	-2.12	-1.90	-1.87		3	-1.26	-1.24	-1.26
Acrylic 0.16	1	-7.47	-6.76	-6.93	**Acrylic** 0.16	1	-2.68	-2.55	-2.42
	2	-10.28	-10.86	-9.68		2	-2.46	-2.49	-2.63
	3	-6.03	-6.33	-5.57		3	-1.29	-1.27	-1.24
Wood 0.41	1	-5.26	-5.36	-5.34	**Wood** 0.41	1	-3.51	-3.15	-3.02
	2	-5.62	-5.46	-5.51		2	-2.90	-3.12	-2.99
	3	-9.36	-8.27	-7.36		3	-3.64	-3.14	-3.13
Polymer Resin 0.90	1	+0.66	+0.54	+0.64	**Polymer Resin** 0.90	1	+0.58	+0.48	+0.48
	2	+0.49	+0.41	+0.45		2	+0.18	+0.31	+0.31
	3	+0.21	+0.22	+0.18		3	+0.48	+0.48	+0.47
Metal 0.05	1	-12.53	-10.30	-8.56	**Metal** 0.05	1	-3.50	-3.29	-3.08
	2	-8.94	-7.86	-7.60		2	-3.20	-3.10	-3.11
	3	-10.54	-9.91	-8.33		3	-2.92	-2.80	-2.79
Ceramic 0.50	1	-0.42	-0.38	-0.32	**Ceramic** 0.50	1	-0.26	-0.21	-0.10
	2	-0.88	-0.83	-0.75		2	-0.30	-0.10	-0.12
	3	-0.57	-0.54	-0.58		3	-0.25	-0.18	-0.09

Humidity Measurements

Humidity affects the generation of electrostatic charges both on the molecular and macroscopic level [19]. In electrostatic precipitators, it has been shown that collection efficiency of small particles (<50 μm) increases with increasing humidity, and that negative corona discharge is less sensitive to humidity than positive [20]. The effects of humidity were examined on three swabs. They were held in air over a 3-min time period (Figures 1.10, 1.11, 1.12). In the 0% RH-30% RH regime there was little change in the initial magnitude; the decay was less than 1 kV; however, in the 50% RH and 80% RH regime, a significant drop in initial magnitude was observed. This was consistent with literature reports that at low levels of humidity, the charges are inserted directly into the bulk volume, whereas if moisture can accumulate on the surface of the material, the charge decays slowly into the bulk [21].

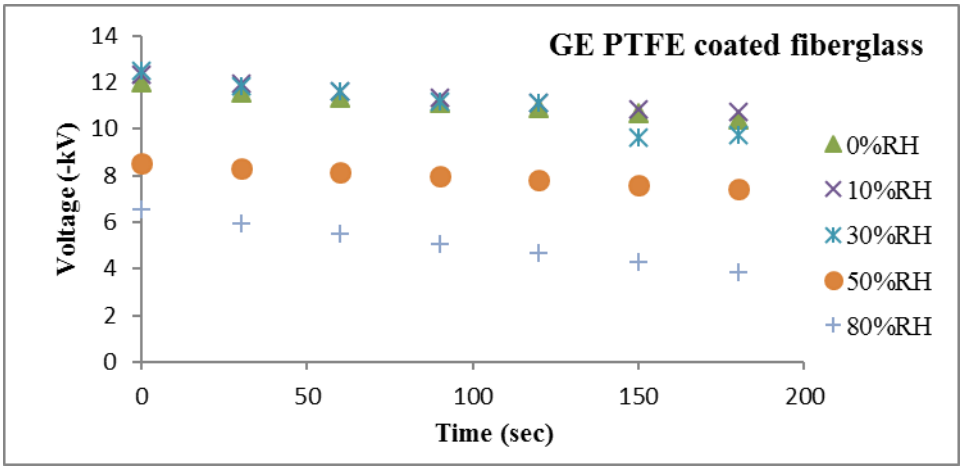

Figure 1.10. PTFE-coated fiberglass swab effective voltage with increasing humidity

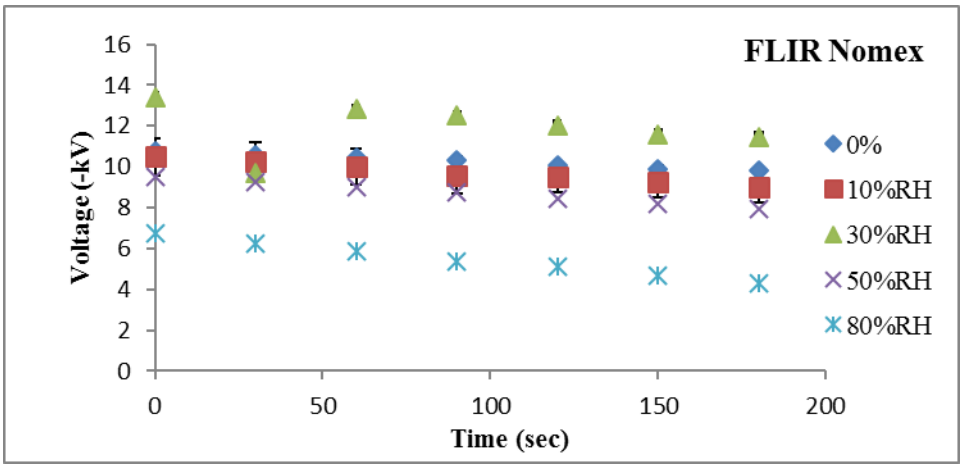

Figure 1.11. FLIR Nomex swab effective voltage with increasing humidity

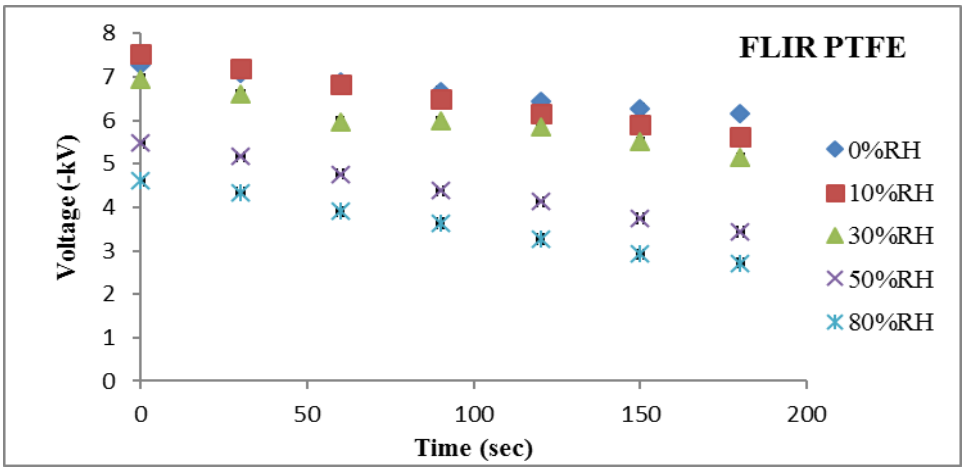

Figure 1.12. FLIR PTFE swab effective voltage with increasing humidity

With cotton swabs, it was difficult to achieve and maintain a negative charge. This we attribute to the position of cotton on the triboelectric series (Figure 1.2). Three cotton swabs were charged at 30% RH and held in air over a three-minute period. The charge on the swab grew more positive with time (Figure 1.13).

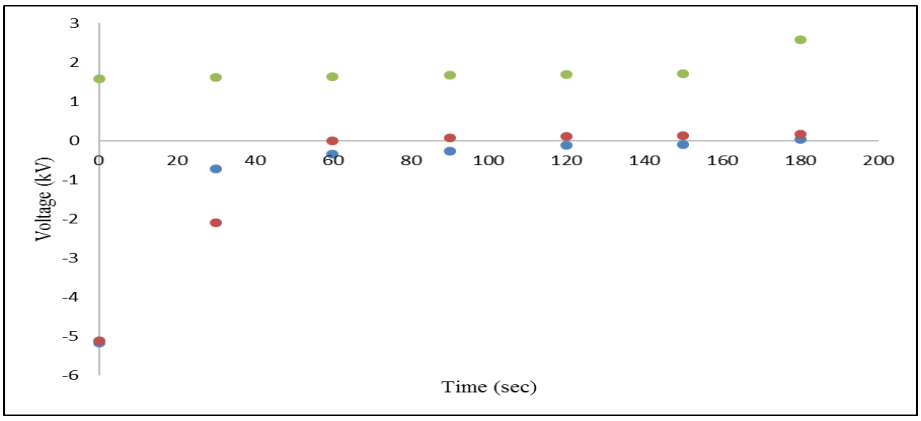

Figure 1.13. DSA Cotton swab held at 30%RH positively charged over 3 minutes

In addition to observing charge retention on the swab with various RH, pickup efficiency was also examined using sucrose and ground glass. Humidity had little effect on the pickup of the ground glass by the PTFE swabs; but sucrose pickup was greater at high RH than at low, contrary to our expectations (Figure 1.14). While high RH reduced charge accumulation on the swab (Figures 1.9, 1.10, 1.11), the increased pickup of sucrose may be related to its solubility in water.

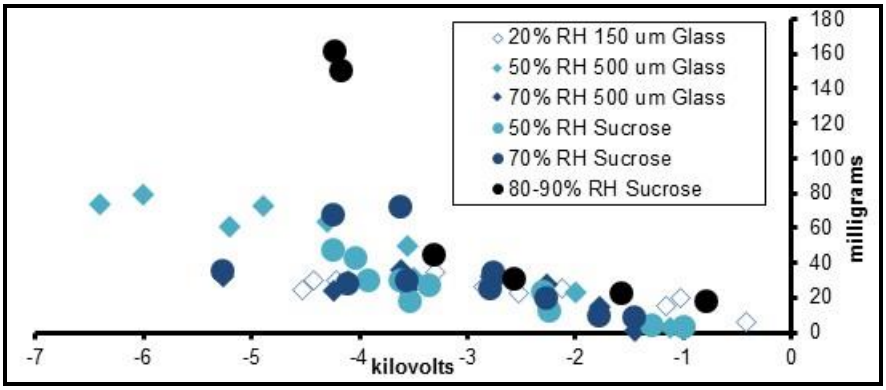

Figure 1.14. Mass pickup of sucrose & ground glass at increasing humidity a voltage

Swabbing and Swab Preparation

For contact swabs, they were physically rubbed against the substrate with the experimenter attempting to apply ~7 N of force [22-23]. Electrostatically enhanced swabs were charged by the inductive charging method and then passed along the substrate from a distance of ~10 mm.

Charging and storage of swabs in stacked and unstacked configuration

Commercially purchased swabs are packaged in multi-swab packages. In order to determine if swabs could be packaged charged or if charging of multiple swabs could occur concurrently, studies were performed examining mass charging and storage of swabs. Attempts to charge (-20 kV for 5 seconds) in a stacked configuration, resulted in only the top swab, i.e. about 2 inches from the pinner, being charged, negatively; the entire 10-swab stack was not charged. This was true for 5-swab, 4-swab and 3-swab stacks. In a 2-swab stack both swabs were charged. For one set of measurements (Table 1.6 -left), the 2-swab stack was picked up together and pulled apart prior to measurement of the charge. This left the top swab charged negatively and the bottom swab charged positively. In a second test, (Table 1.6-right), the 2-swab stack was separated while the bottom swab remained in contact with the aluminum foil; however, charge measurement on both the top and bottom swabs were performed as the swab was held in air. The results suggest that transfer of charge can occur during swab separation.

Table 1.6. Two-swab stack charged together & separated after lifting together in air (left) or separated with one remained in surface contact (right) (experiment performed in triplicate)

top (kV)	-11.05	-11.97	-17.55
bottom (kV)	4.96	4.98	9.84

top (kV)	-7.85	-8.41	-9.44
bottom (kV)	-6.43	-6.54	-5.21

In another experiment, tests were performed (trial 1 at 40% RH and Trial 2 at 30% RH) in which 10 Nomex or 10 PTFE swabs were charged simultaneously at -20 kV for 5 seconds in an unstacked configuration as shown in Figure 1.15. They were stored individually or in stacks of 10 or 5 for 24 hours on aluminum foil. The initial position of the swabs (Figure 1.15) did not have a significant effect on initial charge of the swabs. The Nomex had a higher charge than the PTFE (Tables 1.7 and 1.8).

Figure 1.15. Arrangement of swabs charged simultaneously from 2 inches height

A trial of 10 swabs were placed, individually, 24 hours at 22°C; and another trial of 10 were stored stacked on aluminum foil. For swabs left unstacked, the voltage decay was negligible during that 24-hour period; for swabs stored in a stack, the change in charge varied wildly. Acknowledging that like charges repel, over 24 hours, the charges on Nomex migrated through the swab stack to create a large charge separation. However, for the PTFE stack, the bottom and top swabs are positively charged with the largest absolute difference in charge. In the replicate experiments, there was still much variation in charge created and retained. After 24 hours of storage, in all cases, the top swab of a 10-swab stack had experienced the most change in charge and was more positively charged than the bottom swab. When the storage stack size was reduced from 10 swabs to five, the same trends were observed as with

the 10-swab stack, i.e. the top swab experienced the largest change in charge and was the most positively charged of the stack after 24 hours Table 1.9.

Table 1.7. Nomex swab charged inductively & stored stacked on Al foil for 24 hr

	Trial 1					Trial 2			
	swab	initial charge (kV)	charge at 24 hours (kV)	absolute difference		swab	initial charge (kV)	charge at 24 hours (kV)	absolute difference
bottom -->	1	-10.71	-12.49	1.78	bottom -->	21	-9.46	-0.87	8.59
	2	-6.57	-2.46	4.11		22	-13.32	-1.18	12.14
	3	-11.48	-5.69	5.79		23	-11.40	-8.07	3.33
	4	-10.3	-5.72	4.58		24	-12.69	-7.89	4.80
	5	-11.41	2.03	13.44		25	-12.57	-3.76	8.81
	6	-7.87	-2.82	5.05		26	-13.7	-1.47	12.23
	7	-11.69	5.25	16.94		27	-10.80	-5.24	5.56
	8	-11.66	-5.95	5.71		28	-9.46	4.53	13.99
	9	-11.2	-2.32	8.88		29	-12.04	3.86	15.90
top -->	10	-10.85	7.06	17.91	top -->	30	-11.24	7.95	19.19

Table 1.8. PTFE swab charged inductively & stored stacked on Al foil for 24 hr

	Trial 1					Trial 2			
	swab	initial charge (kV)	charge at 24 hours (kV)	absolute difference		swab	initial charge (kV)	charge at 24 hours (kV)	absolute difference
bottom -->	1	-2.21	5.48	7.69	bottom -->	40	-2.32	2.99	5.31
	2	-5.32	-3.99	1.33		39	-4.92	-2.63	2.29
	3	-4.99	-1.73	3.26		38	-4.46	-2.40	2.06
	4	-4.37	1.03	5.4		37	-3.27	-1.73	1.54
	5	-3.68	-2.1	1.58		36	-3.95	-0.67	3.28
	6	-3.58	-1.51	2.07		35	-2.54	0.20	2.74
	7	-5.05	-3.54	1.51		34	-5.12	0.24	5.36
	8	-5.52	-1	4.52		33	-5.32	1.75	7.07
	9	-4.89	-3.87	1.02		32	-4.68	0.94	5.62
top -->	10	-3.83	9.37	13.2	top -->	31	-3.79	7.61	11.40

Table 1.9. Nomex swabs inductively charged & stored stack on Al foil for 24 hr

	initial charge (kV)	charge at 24 hours (kV)	initial charge (kV)	charge at 24 hours (kV)	initial charge (kV)	charge at 24 hours (kV)
Bottom	-13.02	3.41	-11.14	4.02	-12.22	5.39
	-13.14	-1.96	-12.25	-5.19	-11.43	-12.32
	-12.92	-3.52	-10.49	-7.86	-12.69	-8.97
	-11.62	-4.37	-9.65	2.51	-13.22	-3.94
Top	-13.86	10.95	-10.93	6.57	-10.46	9.11

Quantification of Analytes

The remainder of this study examined pickup efficiency of electrostatic swabs compared to contact swabs. Substrates examined are shown in (Figure 1.16).

Al Foil (metal)
PTFE
Vinyl
ABS
Cotton
Polycarbonate (PC)
High Density Polyethylene (HDPE)
Nylon 1000
Ballistic Nylon
Ohio Zipper
Cardboard
Packing Tape
Bytac®

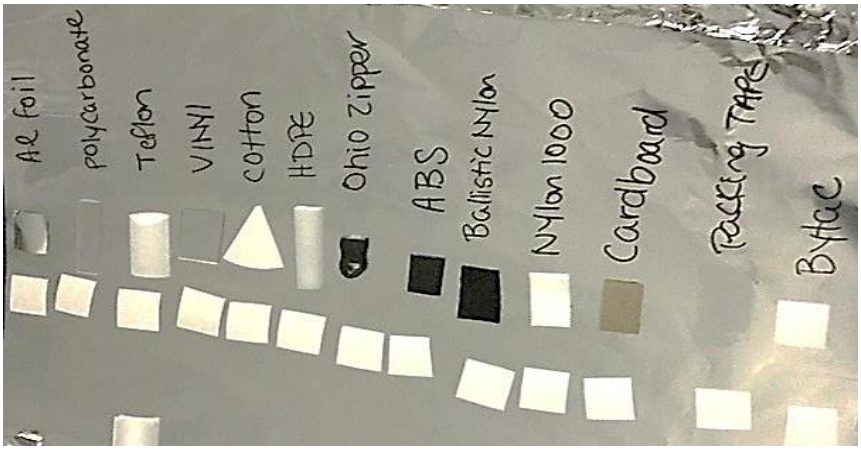

Figure 1.16. Substrates used in this study

The experiment to examine pickup from each substrate was conducted in three parts. First, to determine the extraction efficiency from each substrate, three substrates were directly spiked with 500 ng of analyte in solvent; the solvent was allowed to evaporate; the substrates were extracted with another solvent; the solvent was adjusted to proper volume; and a portion was analyzed by LC/MS. The result indicated the amount of the original 500 ng of explosive that could be recovered from the surface of a given substrate. An example of this using polycarbonate (PC) as substrate S1 is shown in top 3 lines Table 1.10.

Then six samples of Bytac® were spiked with 500 ng of the analyte and rubbed against substrate the first substrate S2 and both S1 and S2 were analyzed to the dry transfer efficiency for a given substrate (middle section of Table 1.10). Three of these S2 and the three S1 against which they were rubbed (dry transferred) and were

extracted with solvent; the solvent was adjusted to proper volume, and was analyzed by LC/MS. The result indicated the amount of explosive that could possibly be transferred from S2 to the swab. That amount plus that remaining on S1 ideally would add to 500 ng (1, middle section). Then, six more Bytac® (S1) were directly spiked with 500 ng of analyte, dry transferred to S2, then three of the S2 were swabbed by contact, i.e. directly rubbing the Nomex swab against S2 (~7 N force) and three of the S2 were swabbed using the electrostatically enhanced Nomex swabs.

Then, these six swabs, S2, and S1 were extracted with solvent; the solvent was adjusted to proper volume; and a portion was analyzed by LC/MS. For any given set, the amount of explosive left on S1 and S2 and found on the swab should have added to 500 ng. The amount of explosive found on the three electrostatically enhanced swabs versus the three contact swabs is shown in Table 1.10 (bottom section) along with percent recovery. A metric of success is labeled Percent Recovery where the nanograms of analyte on the swab (contact or electrostatic) are divided by the total amount of nanograms recovered from 500 ng and displayed as a percentage. For example, in the last line of Table 1.10, 351 ng were found on the swab out of a total recovery of 475 ng. This translates to a 74% recovery.

Polycarbonate

The results shown in Table 1.10 for both contact and electrostatic swabs are below 100 ng, except for one outlier (3rd electrostatic swab). These results suggest analyte on polycarbonate is difficult to sorb onto a swab, whether contact or electrostatic. This could be related to the smoothness of the polycarbonate surface.

Table 1.10. Nomex contact & electrostatic swabbing for PETN from polycarbonate
Electrostatic swabs charged to -8.99 kV, -10.23 kV, & -13.01 kV at RH 25%.
PETN was deposited from a solution of acetone

Substrate (S1) for direct deposit	Substrate (S2) onto which dry transfer	ng PETN out of 500ng
Polycarbonate	--	424
Polycarbonate	--	413
Polycarbonate	--	328

Substrate (S1) for direct deposit	Substrate (S2) onto which dry transfer	remaining on S1	remaining on S2	Total ng PETN recovered from 500 ng
Bytac	Polycarbonate	228	267	495
Bytac	Polycarbonate	312	136	448
Bytac	Polycarbonate	13	372	385

Substrate (S1) for direct deposit	Substrate (S2) onto which dry transfer	remaining on S1	remaining on S2	ng PETN on Nomex by CONTACT swabbing	ng PETN on Nomex by ELECTROSTATIC swabbing	Total ng PETN recovered from 500 ng	Percent Recovery %
Bytac	Polycarbonate	326	160	95		581	16
Bytac	Polycarbonate	114	281	44		439	10
Bytac	Polycarbonate	99	212	41		352	12
Bytac	Polycarbonate	228	155		92	475	19
Bytac	Polycarbonate	74	269		86	429	20
Bytac	Polycarbonate	13	111		351	475	74

Cardboard

The electrostatic swabs outperformed contact with an average pickup efficiency of 39% versus 13% for contact (Table 1.11).

Table 1.11. Nomex contact and electrostatic swabbing for PETN from cardboard
Electrostatic swabs charged to -7.32 kV, -9.65 kV, & -9.89 kV at RH 30%.
PETN was deposited from a solution of acetone

Substrate (S1) for direct deposit	Substrate (S2) onto which dry transfer	ng PETN out of 500ng
Cardboard	--	478
Cardboard	--	440
Cardboard	--	508

Substrate (S1) for direct deposit	Substrate (S2) onto which dry transfer	remaining on S1	remaining on S2	Total ng PETN recovered from 500 ng
Bytac	Cardboard	7	363	370
Bytac	Cardboard	2	481	483
Bytac	Cardboard	3	396	399

Substrate (S1) for direct deposit	Substrate (S2) onto which dry transfer	remaining on S1	remaining on S2	ng PETN on Nomex by CONTACT swabbing	ng PETN on Nomex by ELECTROSTATIC swabbing	Total ng PETN recovered from 500 ng	Percent Recovery %
Bytac	Cardboard	24	372	43		438	10
Bytac	Cardboard	14	367	50		431	12
Bytac	Cardboard	6	338	75		419	18
Bytac	Cardboard	6	417		59	482	12
Bytac	Cardboard	19	132		166	317	52
Bytac	Cardboard	74	192		300	566	53

Bytac®

The average total recovery was low but the electrostatically enhanced swab recovered more PETN than the contact swabs (Table 1.12).

Table 1.12. Nomex contact and electrostatic swabbing for PETN from Bytac®
Electrostatic swabs charged to -8.17 kV, -9.37 kV& -10.28 kV at RH 5%.
PETN was deposited from a solution of acetone

Substrate (S1) for direct deposit	Substrate (S2) onto which dry transfer	ng PETN out of 500ng
Bytac	--	486
Bytac	--	526
Bytac	--	483

Substrate (S1) for direct deposit	Substrate (S2) onto which dry transfer	remaining on S1	remaining on S2	Total ng PETN recovered from 500 ng
Bytac	Bytac	408	26	434
Bytac	Bytac	311	244	555
Bytac	Bytac	279	261	540

Substrate (S1) for direct deposit	Substrate (S2) onto which dry transfer	remaining on S1	remaining on S2	ng PETN on Nomex by CONTACT swabbing	ng PETN on Nomex by ELECTROSTATIC swabbing	Total ng PETN recovered from 500 ng	Percent Recovery %
Bytac	Bytac	439	22	7		468	2
Bytac	Bytac	291	44	15		350	4
Bytac	Bytac	360	52	10		421	2
Bytac	Bytac	383	62		20	465	4
Bytac	Bytac	123	212		108	444	24
Bytac	Bytac	168	50		123	340	36

Acrylonitrile Butadiene Styrene (ABS)

ABS is a common material for hard-sided baggage. Electrostatically enhanced swabs picked up more PETN than contact swabs Table 1.13.

Table 1.13. Nomex contact and electrostatic swabbing for PETN from ABS Electrostatic swabs charged to -7.89 kV, -9.21 kV, & -10.24 kV at RH 35%. PETN was deposited from a solution of isopropanol

Substrate (S1) for direct deposit	Substrate (S2) onto which dry transfer	ng PETN out of 500ng
ABS	--	424
ABS	--	362
ABS	--	450

Substrate (S1) for direct deposit	Substrate (S2) onto which dry transfer	remaining on S1	remaining on S2	Total ng PETN recovered from 500 ng
Bytac	ABS	96	450	546
Bytac	ABS	83	448	531
Bytac	ABS	39	389	429

Substrate (S1) for direct deposit	Substrate (S2) onto which dry transfer	remaining on S1	remaining on S2	ng PETN on Nomex by CONTACT swabbing	ng PETN on Nomex by ELECTROSTATIC swabbing	Total ng PETN recovered from 500 ng	Percent Recovery %
Bytac	ABS	68	284	104		456	23
Bytac	ABS	224	170	70		464	15
Bytac	ABS	185	98	154		438	35
Bytac	ABS	72	297		158	526	30
Bytac	ABS	203	113		208	524	40
Bytac	ABS	16	128		315	459	69

PTFE

Using PTFE as a substrate, electrostatic-enhanced non-contact swabs exhibited better pickup than the contact swab (Table 1.14). PTFE is known for it 'non-stick' properties. This property is so effective that some of the solvent deposited PETN slipped off the substrate, which explained often poor recovery. The recovery was much better for TNT, Table 1.15. The electrostatically enhanced swabs outperformed contact swabbing. TNT is less crystalline than PETN and tends to adhere to surfaces more effectively than PETN.

Table 1.14. Nomex contact and electrostatic swabbing for PETN from PTFE
Electrostatic swabs charged to -8.03 kV, -10.11 kV, and -11.36 kV at RH 25%.
PETN was deposited from a solution of acetone

Substrate (S1) for direct deposit	Substrate (S2) onto which dry transfer	ng PETN out of 500ng
PTFE	--	7
PTFE	--	251
PTFE	--	186

Substrate (S1) for direct deposit	Substrate (S2) onto which dry transfer	remaining on S1	remaining on S2	Total ng PETN recovered from 500 ng
Bytac	PTFE	322	94	416
Bytac	PTFE	334	150	484
Bytac	PTFE	366	157	523

Substrate (S1) for direct deposit	Substrate (S2) onto which dry transfer	remaining on S1	remaining on S2	ng PETN on Nomex by CONTACT swabbing	ng PETN on Nomex by ELECTROSTATIC swabbing	Total ng PETN recovered from 500 ng	Percent Recovery %
Bytac	PTFE	326	2	50		378	13
Bytac	PTFE	93	9	90		192	47
Bytac	PTFE	183	2	43		228	19
Bytac	PTFE	357	2		57	417	14
Bytac	PTFE	381	1		100	482	21
Bytac	PTFE	58	21		140	219	64

Table 1.15. Nomex contact and electrostatic swabbing for TNT from PTFE
Electrostatic swabs charged to -7.41 kV, -10.28 kV, & -8.56 kV at RH 30%.
TNT was deposited from a solution of acetone

Substrate (S1) for direct deposit	Substrate (S2) onto which dry transfer	ng TNT out of 500ng
PTFE	--	467
PTFE	--	427
PTFE	--	423

Substrate (S1) for direct deposit	Substrate (S2) onto which dry transfer	remaining on S1	remaining on S2	Total ng TNT recovered from 500 ng
Bytac	PTFE	140	254	393
Bytac	PTFE	122	278	400
Bytac	PTFE	144	300	444

Substrate (S1) for direct deposit	Substrate (S2) onto which dry transfer	remaining on S1	remaining on S2	ng TNT on Nomex by CONTACT swabbing	ng TNT on Nomex by ELECTROSTATIC swabbing	Total ng TNT recovered from 500 ng	Percent Recovery %
Bytac	PTFE	114	274	66		454	15
Bytac	PTFE	104	247	44		395	11
Bytac	PTFE	175	199	31		405	8
Bytac	PTFE	59	292		41	392	10
Bytac	PTFE	98	174		118	390	30
Bytac	PTFE	92	227		82	401	20

High Density Polyethylene (HDPE)

HDPE, a very smooth plastic; thus, Bytac® did not efficiently transfer the analyte to it. Data in Table 1.16 indicates that the electrostatic swabs slightly outperformed the contact swabs. In the TNT study, Table 1.17, results were similar.

Table 1.16. Nomex contact and electrostatic swabbing for PETN from HDPE
Electrostatic swabs charged to -10.23 kV, -8.41 kV, & -8.55 kV at RH 40%.
PETN was deposited from a solution of acetone

Substrate (S1) for direct deposit	Substrate (S2) onto which dry transfer	ng PETN out of 500ng
HDPE	--	418
HDPE	--	456
HDPE	--	426

Substrate (S1) for direct deposit	Substrate (S2) onto which dry transfer	remaining on S1	remaining on S2	Total ng PETN recovered from 500 ng
Bytac	HDPE	146	289	435
Bytac	HDPE	133	185	318
Bytac	HDPE	165	233	398

Substrate (S1) for direct deposit	Substrate (S2) onto which dry transfer	remaining on S1	remaining on S2	ng PETN on Nomex by CONTACT swabbing	ng PETN on Nomex by ELECTROSTATIC swabbing	Total ng PETN recovered from 500 ng	Percent Recovery %
Bytac	HDPE	151	122	142		415	34
Bytac	HDPE	221	52	154		426	36
Bytac	HDPE	99	127	95		321	30
Bytac	HDPE	22	16		281	319	88
Bytac	HDPE	81	217		127	425	30
Bytac	HDPE	73	196		186	455	41

Table 1.17. Nomex contact and electrostatic swabbing for TNT from HDPE
Electrostatic swabs charged to -9.23 kV, -8.74 kV, and -10.16 kV at RH 40%.
TNT was deposited from a solution of acetone

Substrate (S1) for direct deposit	Substrate (S2) onto which dry transfer	ng TNT out of 500ng
HDPE	--	441
HDPE	--	499
HDPE	--	491

Substrate (S1) for direct deposit	Substrate (S2) onto which dry transfer	remaining on S1	remaining on S2	Total ng TNT recovered from 500 ng
Bytac	HDPE	57	475	532
Bytac	HDPE	90	363	453
Bytac	HDPE	0	443	443

Substrate (S1) for direct deposit	Substrate (S2) onto which dry transfer	remaining on S1	remaining on S2	ng TNT on Nomex by CONTACT swabbing	ng TNT on Nomex by ELECTROSTATIC swabbing	Total ng TNT recovered from 500 ng	Percent Recovery %
Bytac	HDPE	0	42	354		397	89
Bytac	HDPE	78	40	354		472	75
Bytac	HDPE	95	180	205		480	43
Bytac	HDPE	93	119		294	507	58
Bytac	HDPE	92	30		394	516	76
Bytac	HDPE	0	65		355	420	84

Cotton

Direct contact swabbing of cotton was compared to electrostatic swabbing using the standard dry-transfer technique and inductive charging method. Three analytes were examined: PETN (Table 1.18), TNT (Table 1.19), and RDX (Table 1.20). Pickup efficiency is on the order of 20 to 30%. This suggested that the electrostatic swabbing pickup is less dependent on analyte and more dependent on the surface of a substrate.

Table 1.18. Nomex contact and electrostatic swabbing for PETN from cotton
Electrostatic swabs charged to -12.34 kV, -11.49 kV, & -13.69 kV at RH 25%.
PETN was deposited from a solution of acetone

Substrate (S1) for direct deposit	Substrate (S2) onto which dry transfer	ng PETN out of 500ng
Cotton	--	421
Cotton	--	414
Cotton	--	426

Substrate (S1) for direct deposit	Substrate (S2) onto which dry transfer	remaining on S1	remaining on S2	Total ng PETN recovered from 500 ng
Bytac	Cotton	21	507	529
Bytac	Cotton	5	435	439
Bytac	Cotton	1	397	399

Substrate (S1) for direct deposit	Substrate (S2) onto which dry transfer	remaining on S1	remaining on S2	ng PETN on Nomex by CONTACT swabbing	ng PETN on Nomex by ELECTROSTATIC swabbing	Total ng PETN recovered from 500 ng	Percent Recovery %
Bytac	Cotton	1	337	74		412	18
Bytac	Cotton	0	304	51		355	15
Bytac	Cotton	12	297	71		381	19
Bytac	Cotton	20	411		90	521	17
Bytac	Cotton	30	307		154	490	31
Bytac	Cotton	2	334		204	540	38

Table 1.19. Nomex contact and electrostatic swabbing for TNT from cotton
Electrostatic swabs charged to -8.99 kV, -10.23 kV, & -11.14 kV at RH 35%.
TNT was deposited from a solution of acetone

Substrate (S1) for direct deposit	Substrate (S2) onto which dry transfer	ng TNT out of 500ng
Cotton	--	480
Cotton	--	578
Cotton	--	548

Substrate (S1) for direct deposit	Substrate (S2) onto which dry transfer	remaining on S1	remaining on S2	Total ng TNT recovered from 500 ng
Bytac	Cotton	28	448	476
Bytac	Cotton	0	489	489
Bytac	Cotton	14	443	457

Substrate (S1) for direct deposit	Substrate (S2) onto which dry transfer	remaining on S1	remaining on S2	ng TNT on Nomex by CONTACT swabbing	ng TNT on Nomex by ELECTROSTATIC swabbing	Total ng TNT recovered from 500 ng	Percent Recovery %
Bytac	Cotton	0	394	51		445	11
Bytac	Cotton	43	343	92		478	19
Bytac	Cotton	0	344	54		398	14
Bytac	Cotton	0	358		80	438	18
Bytac	Cotton	0	393		53	446	12
Bytac	Cotton	0	355		82	437	19

Table 1.20. Nomex contact and electrostatic swabbing for RDX from cotton
Electrostatic swabs charged to -10.21 kV, -11.44 kV, & -12.66 kV at RH 30%
RDX was deposited from a solution of acetone

Substrate (S1) for direct deposit	Substrate (S2) onto which dry transfer	ng RDX out of 500ng
Cotton	--	535
Cotton	--	460
Cotton	--	434

Substrate (S1) for direct deposit	Substrate (S2) onto which dry transfer	remaining on S1	remaining on S2	Total ng RDX recovered from 500 ng
Bytac	Cotton	123	367	490
Bytac	Cotton	109	326	435
Bytac	Cotton	76	387	463

Substrate (S1) for direct deposit	Substrate (S2) onto which dry transfer	remaining on S1	remaining on S2	ng RDX on Nomex by CONTACT swabbing	ng RDX on Nomex by ELECTROSTATIC swabbing	Total ng RDX recovered from 500 ng	Percent Recovery %
Bytac	Cotton	127	296	87		510	17
Bytac	Cotton	82	290	98		470	21
Bytac	Cotton	137	252	81		471	17
Bytac	Cotton	140	263		87	490	18
Bytac	Cotton	68	284		126	478	26
Bytac	Cotton	63	307		77	448	17

Ohio Travel Bag Zipper

In comparison to some of the other substrates which are flat surfaces, the Ohio zipper is a small pull tab with many grooves (Figure 1.17). According to the manufacturer, the pull tab is made of a polyurethane resin.

Figure 1.17. Ohio Travel Bag Zipper

The results obtained in Table 1.21 show that electrostatic swabs outperformed contact swabbing for PETN. In the TNT study, the dry transfer was less efficient than in the PETN study, though the outcome remained the same with electrostatic swabs outperforming contact (Table 10.22). In the RDX study, to a lesser extent electrostatic swabs outperformed contact (Table 10.23). The third contact swab did not have a sufficient dry transfer which may have skewed the results. Despite the many grooves of the pull tab, standard deviation of percent recovery was quite consistent amongst the three analytes.

Table 1.21. Nomex contact and electrostatic swabbing for PETN from Ohio Zipper
Electrostatic swabs charged to -11.14 kV, -9.43 kV, & -10.87 kV at RH 30%
PETN was deposited from a solution of acetone

Substrate (S1) for direct deposit	Substrate (S2) onto which dry transfer	ng PETN out of 500ng
Ohio Zipper	--	477
Ohio Zipper	--	441
Ohio Zipper	--	461

Substrate (S1) for direct deposit	Substrate (S2) onto which dry transfer	remaining on S1	remaining on S2	Total ng PETN recovered from 500 ng
Bytac	Ohio Zipper	87	363	450
Bytac	Ohio Zipper	35	489	524
Bytac	Ohio Zipper	69	483	552

Substrate (S1) for direct deposit	Substrate (S2) onto which dry transfer	remaining on S1	remaining on S2	ng PETN on Nomex by CONTACT swabbing	ng PETN on Nomex by ELECTROSTATIC swabbing	Total ng PETN recovered from 500 ng	Percent Recovery %
Bytac	Ohio Zipper	62	256	99		417	24
Bytac	Ohio Zipper	19	148	249		416	60
Bytac	Ohio Zipper	1	338	129		469	28
Bytac	Ohio Zipper	1	198		275	474	58
Bytac	Ohio Zipper	9	301		129	440	29
Bytac	Ohio Zipper	3	189		242	433	56

Table 1.22. Nomex contact and electrostatic swabbing for TNT from Ohio Zipper
Electrostatic swabs charged to -7.55 kV, -10.13 kV, &-9.61 kV at RH 30%
TNT was deposited from a solution of acetone

Substrate (S1) for direct deposit	Substrate (S2) onto which dry transfer	ng TNT out of 500ng
Ohio Zipper	--	429
Ohio Zipper	--	545
Ohio Zipper	--	478

Substrate (S1) for direct deposit	Substrate (S2) onto which dry transfer	remaining on S1	remaining on S2	Total ng TNT recovered from 500 ng
Bytac	Ohio Zipper	94	411	505
Bytac	Ohio Zipper	106	369	475
Bytac	Ohio Zipper	78	469	547

Substrate (S1) for direct deposit	Substrate (S2) onto which dry transfer	remaining on S1	remaining on S2	ng TNT on Nomex by CONTACT swabbing	ng TNT on Nomex by ELECTROSTATIC swabbing	Total ng TNT recovered from 500 ng	Percent Recovery %
Bytac	Ohio Zipper	103	257	139		499	28
Bytac	Ohio Zipper	72	265	133		470	28
Bytac	Ohio Zipper	92	258	164		514	32
Bytac	Ohio Zipper	92	260		165	517	32
Bytac	Ohio Zipper	44	264		202	510	40
Bytac	Ohio Zipper	59	249		189	497	38

Table 1.23. Nomex contact and electrostatic swabbing for RDX from Ohio Zipper
Electrostatic swabs charged to -12.61 kV, -10.47 kV, & -7.36 kV at RH 30%
RDX was deposited from a solution of acetone

Substrate (S1) for direct deposit	Substrate (S2) onto which dry transfer	ng RDX out of 500ng
Ohio Zipper	--	540
Ohio Zipper	--	556
Ohio Zipper	--	426

Substrate (S1) for direct deposit	Substrate (S2) onto which dry transfer	remaining on S1	remaining on S2	Total ng RDX recovered from 500 ng
Bytac	Ohio Zipper	3	498	502
Bytac	Ohio Zipper	0	389	389
Bytac	Ohio Zipper	16	534	550

Substrate (S1) for direct deposit	Substrate (S2) onto which dry transfer	remaining on S1	remaining on S2	ng RDX on Nomex by CONTACT swabbing	ng RDX on Nomex by ELECTROSTATIC swabbing	Total ng RDX recovered from 500 ng	Percent Recovery %
Bytac	Ohio Zipper	6	314	180		500	36
Bytac	Ohio Zipper	0	274	206		480	43
Bytac	Ohio Zipper	197	157	168		522	32
Bytac	Ohio Zipper	1	217		278	496	56
Bytac	Ohio Zipper	9	295		175	479	37
Bytac	Ohio Zipper	16	308		208	532	39

Aluminum foil

Dry transfer is often claimed to be more representative of actual explosive residue transfer than direct deposit via solvent [18]. To compare the efficiency of dry transfer to direct deposit of an analyte and to compare contact swabbing to non-contact electrostatic swabbing, the following experiments were performed. Aluminum foil was the substrate; PETN, the analyte; and Nomex, the swab. To evaluate just the transfer method, three aluminum substrates were prepared by directly depositing 500 ng of PETN from acetone solution of 100 ng/µL (Table 1.24). An additional three were prepared by first direct depositing the PETN solution onto Bytac® which then was used to dry transfer the PETN onto the aluminum foil (Table 1.25). Both sets of foil were extracted with 1 mL of 50:50 ACN/H_2O and analyzed on the (LC/MS).

While mass balance is closer to 500 ng for direct deposit Table 1.24, swabs did not recover as much PETN in comparison to the dry transfer method in Table 1.25. In addition, electrostatically enhanced swabs performed better in the dry transfer study. This is to be expected as a residue which was direct deposited via solvent can settle in the grooves of a substrate as solvent evaporates. This is in opposition to dry transfer where the analyte tends to adhere to the more exposed surface. In the case of TNT from aluminum foil, Table 1.26 shows that the recovery for electrostatic swabs outperformed contact swabbing. In addition to a higher recovery on the swab, dry transfer was more efficient with almost all of the analyte on Bytac® being transferred to the substrate. Swabs can only pickup what has been transferred to the substrate, so the efficiency of dry transfer is an important metric in these studies. In the RDX study from aluminum foil, the data in Table 1.27 shows an instance where contact swabs outperformed electrostatic swabs. A high total recovery of RDX on the first contact swab, 58% (390/676 ng), is suspect.

Table 1.24. Nomex contact and electrostatic swabbing for PETN from Al foil using the direct deposit method
Electrostatic swabs charged to -16.02 kV, -14.91 kV, & -14.01 kV at RH 35%
PETN was deposited from a solution of acetone

Substrate (S1) for direct deposit	ng PETN of 500ng remaining on Al Foil after	ng PETN on Nomex by CONTACT swabbing	ng PETN on Nomex by ELECTROSTATIC swabbing	TotAl Foil ng PETN recovered from 500	Percent Recovery %
Al Foil	304	114		418	27
Al Foil	484	58		542	11
Al Foil	456	41		497	8
Al Foil	393		25	418	6
Al Foil	379		37	416	9
Al Foil	428		43	471	9

Table 1.25. Nomex contact and electrostatic swabbing for PETN from Al foil
Electrostatic swabs charged to -15.99 kV, -12.72 kV, & -13.17 kV at RH 35%
PETN was deposited from a solution of acetone

Substrate (S1) for direct deposit	Substrate (S2) onto which dry transfer	ng PETN out of 500ng
Al Foil	--	429
Al Foil	--	361
Al Foil	--	359

Substrate (S1) for direct deposit	Substrate (S2) onto which dry transfer	remaining on S1	remaining on S2	TotAl Foil ng PETN recovered from 500 ng
Bytac	Al Foil	29	433	462
Bytac	Al Foil	19	434	453
Bytac	Al Foil	97	295	392

Substrate (S1) for direct deposit	Substrate (S2) onto which dry transfer	remaining on S1	remaining on S2	ng PETN on Nomex by CONTACT swabbing	ng PETN on Nomex by ELECTROSTATIC swabbing	TotAl Foil ng PETN recovered from 500	Percent Recovery %
Bytac	Al Foil	52	112	60		224	27
Bytac	Al Foil	72	253	28		353	8
Bytac	Al Foil	39	79	75		193	39
Bytac	Al Foil	106	186		100	392	26
Bytac	Al Foil	44	168		130	342	38
Bytac	Al Foil	55	174		135	364	37

Table 1.26. Nomex contact and electrostatic swabbing for TNT from Al foil
Electrostatic swabs charged to -8.43 kV, -8.87 kV, & -6.24 kV at RH 40%
TNT was deposited from a solution of acetone

Substrate (S1) for direct deposit	Substrate (S2) onto which dry transfer	ng TNT out of 500ng
Al Foil	--	472
Al Foil	--	423
Al Foil	--	425

Substrate (S1) for direct deposit	Substrate (S2) onto which dry transfer	remaining on S1	remaining on S2	Total ng TNT recovered from 500 ng
Bytac	Al Foil	0	534	534
Bytac	Al Foil	0	486	486
Bytac	Al Foil	0	477	477

Substrate (S1) for direct deposit	Substrate (S2) onto which dry transfer	remaining on S1	remaining on S2	ng TNT on Nomex by CONTACT swabbing	ng TNT on Nomex by ELECTROSTATIC swabbing	Total ng TNT recovered from 500 ng	Percent Recovery %
Bytac	Al Foil	0	247	137		384	36
Bytac	Al Foil	16	281	89		386	23
Bytac	Al Foil	11	167	154		332	46
Bytac	Al Foil	0	134		283	417	68
Bytac	Al Foil	8	122		235	365	64
Bytac	Al Foil	0	159		187	346	54

Table 1.27. Nomex contact and electrostatic swabbing for RDX from Al foil
Electrostatic swabs charged to -7.36 kV, -7.99 kV, & -9.11 kV at RH 40%
RDX was deposited from a solution of acetone

Substrate (S1) for direct deposit	Substrate (S2) onto which dry transfer	ng RDX out of 500ng
Al Foil	--	534
Al Foil	--	530
Al Foil	--	540

Substrate (S1) for direct deposit	Substrate (S2) onto which dry transfer	remaining on S1	remaining on S2	Total ng RDX recovered from 500 ng
Bytac	Al Foil	97	438	535
Bytac	Al Foil	102	404	506
Bytac	Al Foil	73	422	495

Substrate (S1) for direct deposit	Substrate (S2) onto which dry transfer	remaining on S1	remaining on S2	ng RDX on Nomex by CONTACT swabbing	ng RDX on Nomex by ELECTROSTATIC swabbing	Total ng RDX recovered from 500 ng	Percent Recovery %
Bytac	Al Foil	89	196	390		676	58
Bytac	Al Foil	36	346	137		519	26
Bytac	Al Foil	0	249	259		508	51
Bytac	Al Foil	79	359		60	499	12
Bytac	Al Foil	53	326		136	515	26
Bytac	Al Foil	50	316		176	542	32

Ballistic Nylon

In the ballistic nylon study, excess methanol >10 mL was necessary to achieve a satisfactory quantification due to its absorption of solvent. The percent recovery in both contact and electrostatic swabbing was low, contact outperformed electrostatic swabs (Table 1.28).

Table 1.28. Nomex contact and electrostatic swabbing for PETN from Ballistic Nylon
Electrostatic swabs charged to -7.16 kV, -6.99 kV, & -9.71 kV at RH 40%
PETN was deposited from a solution of acetone

Substrate (S1) for direct deposit	Substrate (S2) onto which dry transfer	ng PETN out of 500ng
Ballistic Nylon	--	575
Ballistic Nylon	--	626
Ballistic Nylon	--	583

Substrate (S1) for direct deposit	Substrate (S2) onto which dry transfer	remaining on S1	remaining on S2	Total ng PETN recovered from 500 ng
Bytac	Ballistic Nylon	31	460	492
Bytac	Ballistic Nylon	54	473	527
Bytac	Ballistic Nylon	6	445	451

Substrate (S1) for direct deposit	Substrate (S2) onto which dry transfer	remaining on S1	remaining on S2	ng PETN on Nomex by CONTACT swabbing	ng PETN on Nomex by ELECTROSTATIC swabbing	Total ng PETN recovered from 500 ng	Percent Recovery %
Bytac	Ballistic Nylon	15	325	51		391	13
Bytac	Ballistic Nylon	5	305	96		406	24
Bytac	Ballistic Nylon	20	342	80		442	18
Bytac	Ballistic Nylon	4	406		67	477	14
Bytac	Ballistic Nylon	6	406		24	436	5
Bytac	Ballistic Nylon	10	388		33	431	8

Packing Tape

The objective in determining pickup from polypropylene packing tape was to examine the non-sticky side. It was necessary to remove the adhesive backing for subsequent extraction of the analyte. However, no amount of extraction completely removed the adhesive. FTIR analysis (Figure 1.18) revealed the tape was made of polypropylene. Therefore, polypropylene was used as substrate S2. Data in Table 1.29 shows PETN deposited on polypropylene resulted in recoveries <100%.

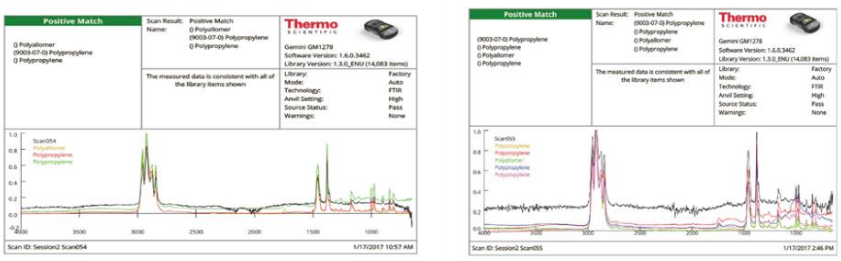

Figure 1.18. FTIR spectrum of authentic packing tape sample (Left) surrogate (Right)

Table 1.29 Nomex contact and electrostatic swabbing for PETN from packing tape
Electrostatic swabs charged to -7.58 kV, -11.52 kV, & -10.31 kV at RH 20%
PETN was deposited from a solution of acetone

Substrate (S1) for direct deposit	Substrate (S2) onto which dry transfer	ng PETN out of 500ng
TAPE	--	120
TAPE	--	24
TAPE	--	67

Substrate (S1) for direct deposit	Substrate (S2) onto which dry transfer	remaining on S1	remaining on S2	Total ng PETN recovered from 500 ng
Bytac	TAPE	160	26	187
Bytac	TAPE	64	114	178
Bytac	TAPE	334	5	339

Substrate (S1) for direct deposit	Substrate (S2) onto which dry transfer	remaining on S1	remaining on S2	ng PETN on Nomex by CONTACT swabbing	ng PETN on Nomex by ELECTROSTATIC swabbing	Total ng PETN recovered from 500 ng	Percent Recovery %
Bytac	TAPE	280	3	25		308	8
Bytac	TAPE	371	12	29		412	7
Bytac	TAPE	130	4	78		212	37
Bytac	TAPE	148	6		52	206	25
Bytac	TAPE	241	5		50	295	17
Bytac	TAPE	429	2		17	447	4

Vinyl/ Nylon 1000

Simulated leather with flannel-backed vinyl, as well as the clear sheeting vinyl, resulted in matrix interference on the LC/MS. The extraction of vinyl in various solvents, acetonitrile, isopropanol, and methanol, decreased the signal response of the analyte, PETN, and gave false values in quantification. It was attempted to extract this matrix, and use the matrix as the solvent, matrix-matched standards, in order to eliminate this issue. The linear regression correlation (R^2) was unacceptable for quantification, so there is no data in quantifying from dry transfer for the vinyl substrate. The same conflict occurred with Nylon 1000, though the black color was extracted in the solvent, and initially this seemed to be the interferent. After obtaining white Nylon 1000 and attempting the same extraction, the interferent was still present. No further attempts to quantify on LC/MS with these substrates occurred in this study.

Explosive Trace Detectors (ETD)

In this section the feasibility of using electrostatic non-contact swabbing methods with airport ETDs is verified. Shown in Figures 1.19 and 1.20 are responses of increasing amounts of PETN to an ion mobility spectrometer in NITRO and PETN response modes. PETN response is hyperbolic, approaching maximum response at higher amounts of PETN. This suggests that the detector is saturated with PETN. Figure 1.21 shows similar results for ammonium nitrate on IMS in NITRO mode.

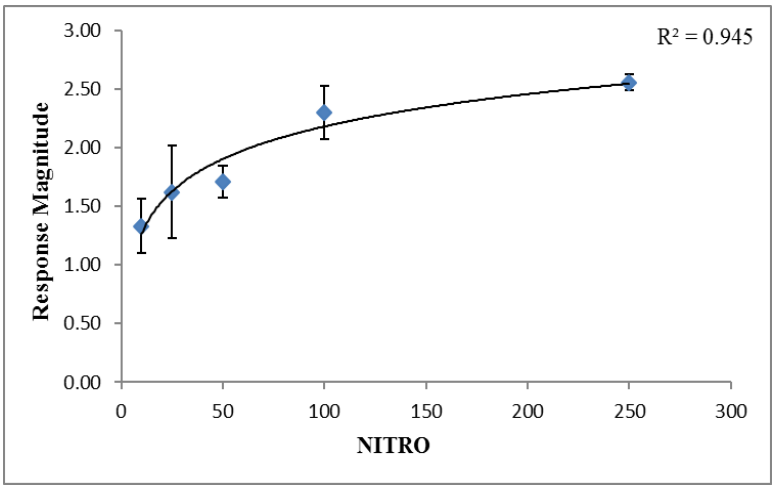

Figure 1.19. IMS signal response for NITRO for increasing concentrations of PETN

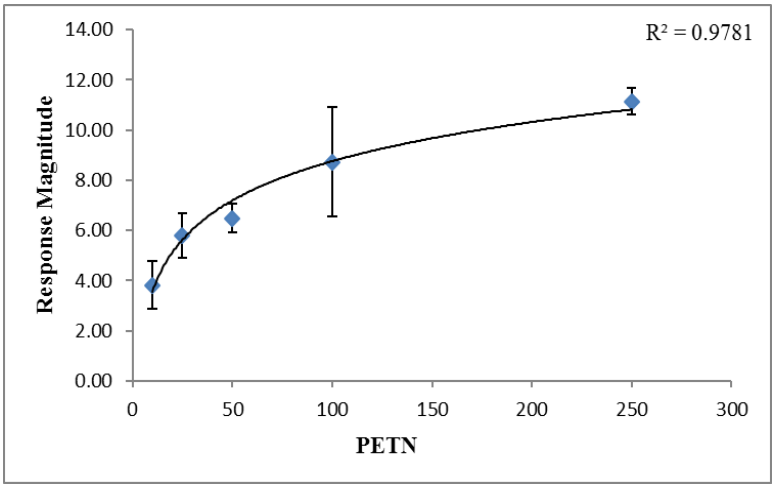

Figure 1.20. IMS signal response for PETN for increasing concentrations of PETN

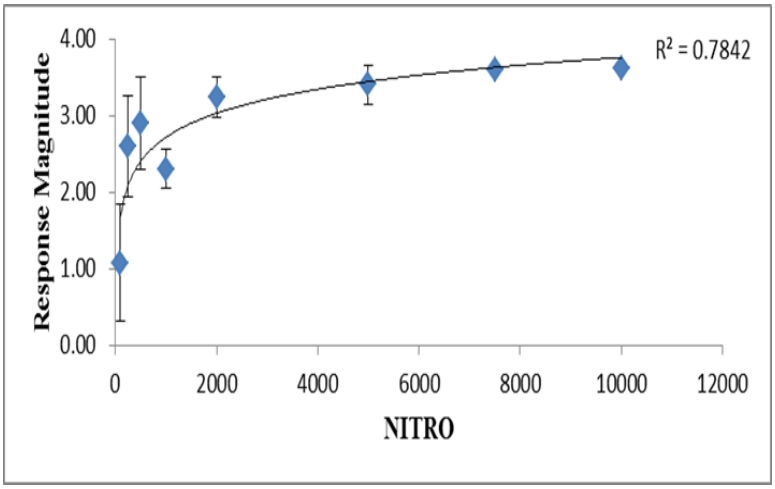

Figure 1.21. IMS signal response for NITRO for increasing concentrations of AN

In Table 1.30, the dry transfer method was used to deposit 100 ng of PETN, 100 ng TNT, or 500 ng AN on the various substrates listed in the substrate 2 column. These substrates were swabbed with either an electrostatically enhanced swab or a contact swab; the swab was presented to the ETD, and the magnitude of the response was recorded.

Table 1.30. IMS responses of contact vs electrostatically enhanced swabs

	PETN Detection						AN Detection				TNT Detection			
Substrate 2	Charge (-kV) or Contact	Alarm type	response	number repeats required	Alarm type	response	Charge (-kV) or Contact	Alarm type	response	number repeats required	Charge (-kV) or Contact	Alarm type	response	number repeats required
HDPE	6.91	PETN	**7.02**	0	NITRO	**1.51**	9.45	NITRO	**2.44**	0	8.01	TNT	**4.27**	0
	Contact	PETN	**1.71**	2			Contact	NITRO	**2.69**	0	Contact	TNT	**4.07**	0
Cotton	5.24	PETN	**4.43**	0	NITRO	**1.13**	10.23	NITRO	**2.31**	0	9.84	TNT	**3.04**	0
	Contact	PETN	**1.42**	2			Contact	NITRO	**1.00**	2	Contact	X	X	3
Al Foil	5.20, 7.64	PETN	**3.76**	2	NITRO	**1.64**	8.31	NITRO	**1.24**	0	6.86	TNT	**2.11**	0
	Contact	PETN	**1.13**	3			Contact	NITRO	**1.03**	1	Contact	X	X	3
Nylon 1000	9.46	PETN	**1.42**	0	NITRO	**1.32**	10.23, 11.17	NITRO	**1.08**	1				
	Contact			2	NITRO	**1.00**	Contact	X	X	3				
PC	7.2, 7.8, 6.5	X	X	3			6.4, 9.9, 7.5	X	X	3				
	Contact	X	X	3			Contact	X	X	3				
Ballistic Nylon	5.8, 5.9, 6.0	X	X	3			7.5, 8.7, 7.1	X	X	3				
	Contact	X	X	3			Contact	X	X	3				
PTFE	5.8, 6.3, 6.0	X	X	3			7.3, 6.5, 9.5	NITRO	X	3				
	Contact	X	X	3			Contact	NITRO	X	3				
ABS	8.53	X	X	3			8.74, 8.53	NITRO	**1.22**	1				
	Contact	X	X	3			Contact	X	X	3				
Vinyl	10.33	PETN	**1.58**	0			6.95, 9.31	NITRO	**2.01**	1				
	Contact	X	X	3			Contact	X	X	3				

The results show electrostatically enhanced swabs achieved higher response magnitudes than contact swabs. In the cases of ballistic nylon, polycarbonate (PC), PTFE, and ABS neither electrostatic nor contact swabbing was able to elicit responses from the instrument at this concentration. This trend agrees with LC/MS quantification showing that neither electrostatic nor contact swabbing had a greatly enhanced performance. In the vinyl and Nylon 1000 experiments, electrostatic swabs retained a higher amount of analyte than contact. Results agree with literature that transfer efficiency is poor to hard plastic [24].

C-4 Fingerprints: Comparing positive and negative voltages

In order to determine if the sign of the voltage had an effect on sorption of explosive residue, a simple test was completed (Table 1.31). With increasing magnitude, whether positive or negative, response magnitude increases, the only outlier being the first test of +4.78 kV where the response magnitude is the highest. Two swabs (fiberglass coated Teflon) were stacked on the grounding plate. The swabs were charged for 5 seconds at -20 kV from 2 inches away from the pinner at 40% RH. Single C-4 fingerprints were made with index fingers of various participants on a cellulose substrate (filter paper). Charges were recorded and swabs approached fingerprints from 10 mm above the substrate. Swabs were tested in the Morpho Itemiser DX ETD. Additionally, controls were performed where charged swabs went directly into the inlet to insure no false alarms came from charging. These results verified that both positive and negative charging results in a response from the IMS.

Table 1.31. Positive and negative charging to pick up RDX from a C-4 fingerprint

CHARGE (KV)	RESPONSE MAGNITUDE
+4.78	4.27 2.67
-10.43	3.92 2.30
+2.79	1.17 0.92
-8.69	2.91 1.42
+6.76	3.88 2.11
CONTROLS WITH NO C4	
+5.05	
-6.39	

CONCLUSION

Commercial swabs were charged using the inductive method. This charging method was optimized for the surface on which charging occurred and length of charging time (5 sec). Several commercial swab types were tested in humidity ranging 0 to 80% RH. As humidity increased charge imparted to the swabs decreased. The negatively charged swabbing material still developed enough charge to enhance particle pickup. Cotton swabs charged positively, and rapidly lost this charge. Storage and stacking methods were tested to determine if swabs could be packaged charged; this did not seem to be the case.

Methods of applying the analyte to the substrate surface were examined. Direct deposit of the analyte from solution with subsequent evaporation of the solvent was compared to the "dry transfer" method. Dry transfer and Nomex swabs were used in all quantitative comparison studies of contact versus non-contact, electrostatic swabbing. Using the dry transfer method, thirteen substrates were analyzed; and analytical protocols, developed to quantify three different organic explosives in comparing contact to electrostatic swabbing. In the case where quantification of the analyte pickup was not amenable to LC methods, a commercial ETD and Teflon-coated fiberglass swabs were used to compare the relative pickup by the two swabbing methods.

Findings, summarized in Tables 1.32 and 1.33 indicate that in most cases, electrostatically enhanced swabs were more effective in collecting explosives particles than contact swabbing. Use of this technique would decrease the invasiveness of swabbing and possibly lower false alarms by eliminating the pickup of some types of

contaminants. It is anticipated at check point, charging would increase sample time by about 5 seconds and that humidity would be similar to that employed in this testing.

Table 1.32. Quantification as % Recoveries comparing pickup of explosives using contact vs electrostatic swabs at 5 to 40% RH

	TNT				**RDX**				PETN			
	C	STD	E	STD	C	STD	E	STD	C	STD	E	STD
Polycarbonate									13	3	38	25
Cardboard									13	4	39	19
Bytac									3	1	22	13
ABS									24	8	46	16
Teflon	11	3	20	8					26	15	33	22
High Density Polyethylene	69	20	73	11					33	3	53	25
Cotton	15	3	16	3	18	2	20	4	17	2	29	8
Zippers	29	3	37	2	37	4	44	8	37	16	48	13
Al Foil (metal)	35	10	62	6	45	13	23	8	29	5	34	5
Packing tape									17	14	15	9
Ballistic Nylon									18	4	9	4
Nylon 1000									ETD			
Vinyl									ETD			

Table 1.33. IMS response comparing pickup of explosives on contact vs electrostatic swabs

	PETN Detection						AN Detection				TNT Detection			
Substrate 2	Charge (-kV) or Contact	Alarm type	response	number repeats required	Alarm type	response	Charge (-kV) or Contact	Alarm type	response	number repeats required	Charge (-kV) or Contact	Alarm type	response	number repeats required
HDPE	7	PETN		0	NITRO		9	NITRO		0	8	TNT		0
	Contact	PETN		2			Contact	NITRO		0	Contact	TNT		0
Cotton	5	PETN		0	NITRO		10	NITRO		0	10	TNT		0
	Contact	PETN		2			Contact	NITRO		2	Contact	X	X	3
Al Foil	7.00	PETN		2	NITRO		8	NITRO		0	7	TNT		0
	Contact	PETN		3			Contact	NITRO		1	Contact	X	X	3
Nylon 1000	9	PETN		0	NITRO		11	NITRO		1				
	Contact			2	NITRO		Contact	X	X	3				
PC	7	X	X	3			8	X	X	3				
	Contact	X	X	3			Contact	X	X	3				
Ballistic Nylon	6	X	X	3			7	X	X	3				
	Contact	X	X	3			Contact	X	X	3				
PTFE	6	X	X	3			9	NITRO	X	3				
	Contact	X	X	3			Contact	NITRO	X	3				
ABS	9	X	X	3			9.00	NITRO		1				
	Contact	X	X	3			Contact	X	X	3				
Vinyl	10	PETN		0			9	NITRO		1				
	Contact	X	X	3			Contact	X	X	3				

response level
high
medium
low

REFERENCES

1. Moore, D. S., Recent Advances in Trace Explosives Detection. *Sense Imaging* **2007**, *8*, 9-38.
2. Verkouteren, J. R.; Coleman, J. L.; Fletcher, R. A.; Smith, W. J.; Klouda, G. A.; Gillen, G., A method to determine collection efficiency of particles by swipe sampling. *Measurement Science and Technology* 2008, *19* (11), 115101.
3. Verkouteren, J.; Grandner, J.; MacIsaac, K.; Ritchie, N.; In *Forensics@NIST* 2012, Gaithersburg, MD, November 29, 2012 Gaithersburg, MD, November 29, 2012. http://www.nist.gov/oles/upload/4-Verkouteren_Jennifer-Surface-Wipe-Sampling.pdf
4. Images Scientific Instruments: Van de Graaf Generator. http://www.imagesco.com/articles/high-voltage/van_de_graaf.html
5. Baytekin, H. T. The Mosaic of Surface Charge in Contact Electrification. Science **2011** 333, 308-312.
6. Williams, M. W. Triboelectric charging of insulators- Mass transfer versus electrons/ions. *Journal of Electrostatics* **2012** 70, 233-234.
7. Diaz, A.F. A semi-quantitative tribo-electric series for polymeric materials: the influence of chemical structure and properties. *Journal of Electrostatics* **2004** 62, 277-290.
8. Pidoll, U. Predicting the electrostatic charging behavior of insulating materials without charging tests. *Journal of Electrostatics* **2013** 71, 513-516.

9. Park, C. H.; Chun B.C. Triboelectric series and charging properties of plastics using the designed vertical-reciprocation charger. *Journal of Electrostatics* **2008** 66, 578-583.
10. Sow, M.; Lacks, D. J. Effects of material strain on triboelectric charging: Influence of material properties. *Journal of Electrostatics* **2013** 71, 396-399.
11. Moreno, R. A.; Gross, B. Measurement of potential buildup and decay, surface charge density, and charging currents of corona-charged polymer foil electrets. *Journal of Applied Physics* **1976** 47, 3397-3402.
12. Sessler, G. M.; Alquie, C.; Lewiner, J. Charge distrubution in Tefon FEP negatively corona charged to high potentials. *Journal of Applied Physics* **1992** 71, 2280-2284.
13. Gutmann, F. The Electret. *Reviews of Modern Physics* **1948** 20, 457-472.
14. Sessler, G. M. Electrets: recent developments. *Journal of Electrostatics* **2001** 51-52, 137-145.
15. Smyth, C.P. Dielectric behavior and structure; dielectric constant and loss, dipole moment and molecular structure, McGraw-Hill, **1955**.
16. Jonassen, N. *Electrostatics*, International Thomson publishing, **1998**.
17. Greenspan, Lewis. Humidity Fixed Points Binary Saturated Aqueous Solutions. *J. Res. Natl. Bur. Stand. Sec. A* **1976** 81A, 89-96.
18. Chamberlin, R; Dry Transfer Method for the Preparation of Explosives Test Samples, US 6470730 B1, October 29, 2002.

19. Nemeth, E; Simon, F. Polymer tribo-electric charging: dependence on thermodynamic surface properties and relative humidity. *Journal of Electrostatics* **2003** 58, 3-16.
20. Nouri, H; Zouzou, N.; Dascalescu, L.; Zebboudj, Y. Investigation of relative humidity effect of particles velocity and collection efficiency of laboratory scale electrostatic precipitator. *Process Safety and Environmental Protection* **2016** 104, 225-232.
21. Yawootti, A.; Intra, P.; Tippayawong, N.; Rattanadecho, P. An experimental study of relative humidity and air flow effects on positive and negative corona discharges in a corona-needle charger. *Journal of Electrostatics* **2015** 77, 116-122.
22. Staymates, M.E.; Grandner, J.; Verkouteren, J. R.; Pressure-Sensitive Sampling Wands for Homeland Security Applications. *IEE Sensors Journal* **2013** 13, 4844-4850.
23. Verkouteren, J. R.; Ritchie, W. M.; Gillen, G.; Use of force-sensing array films to improve surface wipe sampling. *J. Environ. Sci. Process. Impacts* **2013**, 15, 373-380.
24. Tam, M.; Pilon, P.; Zaknoun, H.; Quantified explosives transfer on surfaces for the evaluation of trace detection equipment. *J. Forensic Sci.* **2013**, 58, 5, 1336-1340.

Manuscript 2

Potential Biocides: Polymer Packaging of Iodine containing Pyrotechnics

By Rebecca Levine, Jimmie C. Oxley, James Smith, Matthew Porter, Joe E. Brady IV

Chemistry Department

University of Rhode Island

140 Flagg Road, Kingston, RI 02881

Prepared for submission to Journal of Energetic Materials

ABSTRACT

Iodine-producing pyrotechnics have been investigated as biocides against biological warfare agents [1-4]. For controlled application and dispersion of these formulations in the field, polyurethane matrixes were examined as binders. To that end, five energetic polyols containing energetic moieties nitro ($–NO_2$) and/or azide ($–N_3$) were synthesized and characterized. These were used as partial replacements for triethanolamine (TEOA) in its reaction with toluene diisocyanate (TDI) to produce polyurethane. The most promising of these polyurethane foams were mixed with a pyrotechnic formulation (90/10 $Ca(IO_3)_2$/Al powder) to test for heat and iodine output. Despite high solids loading (>70%) the foam cured without significant decrease in expansion compared to the simple polyurethane (about 9 fold). Without polyurethane, a 90/10 formulation of $Ca(IO_3)_2$/Al resisted ignition, but in the presence of the foam binder it was highly flammable. Addition of the energetic monomer did not greatly improve the excellent heat output of the standard polyurethane foam, but it improved iodine output.

INTRODUCTION

The threat of biological weapons, specifically spores of *Bacillus anthracis* species, are of concern to those charged with homeland security. Although the exact kill mechanism is unknown, current research efforts suggest that heat and iodine gases can act as a biocide causing DNA damage and increasing the kill-rate in spores [3-4]. Previous work examined the heat and iodine outputs of various fuels and oxides of iodine mixtures [5]. For controlled application and dispersion of the biocidal formulations in the field, these fuel/oxidizer mixtures require a binder. For a quick and thorough application of the biocidal formulation, a sprayable binder was considered best. The properties desired in a sprayable binder would include rapid curing (less than 10 seconds) with significant expansion and acceptable mechanical properties so that high solids loading could be achieved. It was determined that polyurethane foams met these needs. Because polyurethane formations are based on combining a diisocyanate with a polyol to produce a urethane linkage, (Figure 2.1) a number of modifications can be applied by changing one of the monomers [6]. Functionalizing polymers with nitro or azide groups is the usual approach to creating energetic binders [7-9]. Polyurethane foams were exclusively investigated in this study.

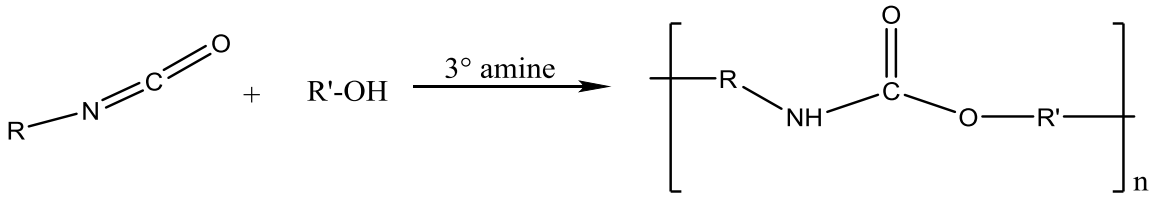

Figure 2.1. general urethane linkage schematic

EXPERIMENTAL METHODS

Materials

All chemical reagents and analytical grade solvents were purchased from, Acros Organics, Alpha Aesar, Fisher Scientific, TCI, or STREM and used without further purification. Particle size of the calcium iodate was 70 to 150 μm; and the aluminum, from Obron, was 23 μm. To lower the surface tension during polymer preparation, promote uniform cell structure, and increase expansion, surfactant (Triton^{TM} GR-7M) provided by DOW Chemical was used at 1 wt % solution in pentane.

Fourier Transform-Infared Spectrometer (FTIR)

Infrared spectra were measured with a Thermo Scientific Nicolet 6700 spectrometer equipped with a Smart iTR diamond ATR. FTIR spectra were recorded at ambient temperature. Background and spectra were collected in ranges of 4000-650 cm^{-1}.

Thermal Measurements

Melting points, decomposition temperatures, and enthalpies were determined using a TA Q100 for differential scanning calorimetry (DSC), calibrated against an indium standard, heating at 20 °C min^{-1} under nitrogen flow of 50 mL/min. Hermetic aluminum pans were used for monomers, and glass sealed capillaries, for polymers. Polymer decomposition was monitored with a TA Q600 Simultaneous DSC/TGA (SDT) instrument; samples were held in open alumina pans, with heating rate 20 °C min^{-1} and nitrogen flow of 300 mL min^{-1}.

Liquid Chromatography/ Mass Spectrometer (LCMS)

To determine mass spectra, each compound was dissolved in methanol to make a 1mg/mL solution and then serially diluted to 10 μg/mL. This methanol solution was

infused into Thermo Scientific LTQ Orbitrap XL™ mass spectrometer (MS) at a rate of 5 µL/min using electrospray ionization source in negative mode. The ionization source and ion optics parameters were as follows: sheath gas 8, auxiliary gas 1, spray voltage 4.0 kV, capillary temperature 275 °C, capillary voltage -1 V, tube lens -33.8 V, multipole 00 offset 2.5 V, lens 0 4.5 V, multipole 0 offset 4.75 V, lens 1 20.0 V, gate lens 64.0 V, multiple 1 offset 8.0 V, multipole RF amplitude 400.0 V, front lens 4.75 V. The mass spectra were collected using a full scan in ranges of 70 to 800 AMU (atomic mass units).

Monomers

2-(Hydroxymethyl)-2-nitropropane-1,3-diol (TMNM, 1) [10]

TMNM (**1**) was prepared by mixing nitromethane (17.9 g, 0.293 mol) in a potassium hydroxide (0.49 g, 8.7 mol) methanol (45 mL)/dichloromethane (2 mL) solution in a 250 mL round-bottom flask. The flask was cooled to 5°C and portions of 28g, 0.933mol paraformaldehyde (37% w/v in water) solution was stirred in over 30 minutes. The mixture was heated to 40°C, refluxed 2 hours, cooled to room temperature, and placed in a freezer overnight. The precipitate was collected by vacuum filtration, washed with hexanes, and dried in vacuum oven overnight at 50 °C to yield Compound **1** 26.81g, 60%, m.p. 150-4°C (Figure 2.2).

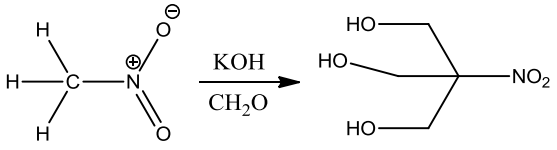

2-(hydroxymethyl)-2-nitropropane-1,3-diol

1

Figure 2.2. Synthesis of 2-(Hydroxymethyl)-2-nitropropane-1,3-diol (TMNM**, 1**)

2,3-Bis(hydroxymethyl)-1,3-dinitrobutane-1,4-diol (TETRA, 2) [10]

Compound **1** was condensed with acetone to form the ketal, (2,2-dimethyl-5-nitro-1,3-dioxan-5-yl)methanol **(2a)**, as follows. In a 250 mL round bottom flask Compound **1** (30.21 g, 0.2 mol) and acetone (36.31 g, 0.620 mol) were combined, stirred, and warmed until Compound **1** was fully dissolved. The mixture was cooled to 20°C in an ice bath, and BF_3 (48% in ether, 34.38 g, 0.243 mol) was added to the flask all at once. The mixture was briefly heated to 60°C (~6 minutes) and then poured into a 2L beaker containing saturated sodium bicarbonate solution (500 mL) and shaved ice (100 mL). The tan colored precipitate was collected by vacuum filtration, washed with water, and air dried to yield 35.07 g (80%) of Compound **2a**, melting point 130-132°C.

The dimerized ketal,2,2,2',2'-tetramethyl-5,5'-dinitro-5,5'-bi(1,3-dioxane) **(2b)**, was prepared from Compound **2a** (57.08 g, 0.3 mol) by placing it in 750 mL water in a 2 L round-bottom flask and heating it at 50°C for 2.5 hours with sodium hydroxide solution (50% w/w, 49 g, 0.6 mol). The mixture was cooled to 20°C; sodium persulfate (146 g, 0.613 mol) was added over the course of an hour; and stirring was continued at room temperature for 24 hours at which time sodium hydroxide solution (50% w/w) was added until the pH reached 11-12. The precipitate was filtered, washed with cold hexanes, and air dried to yield 2,2,2',2'-tetramethyl-5,5'-dinitro-5,5'-bi(1,3-dioxane), (35.05 g, 72% yield), Compound **2b**, a tan solid with melting point of 129-130°C.

The 2,3-bis(hydroxymethyl)-1,3-dinitrobutane-1,4-diol, Compound **2,** was prepared in a 250 mL round-bottom flask by dissolving Compound **2b** (17.2 g, 0.053 mol) in 190 mL of methanol and 15 mL of 12M HCl. The mixture was refluxed at 65°C for 40 minutes before the methanol and HCl were removed by rotary evaporation. The

crude yield was 11.1 g (87%). The crude product compound 2 had a melting point of 100°C. It was recrystallized from 25 mL of hot ethyl acetate; the precipitate was rinsed with hexanes, and dried to yield 2,3-bis(hydroxymethyl)-1,3-dinitrobutane-1,4-diol, compound **2** 8.37 g with a melting point of 108°C (Figure 2.3).

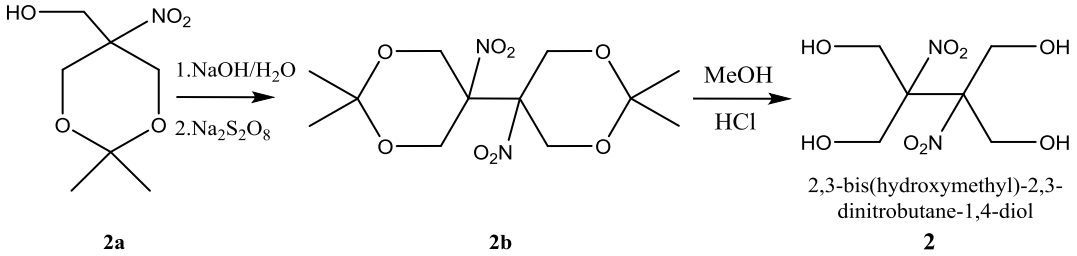

Figure 2.3. Synthesis of 2,3-Bis(hydroxymethyl)-1,3-dinitrobutane-1,4-diol (TETRA, **2**)

2-(Azidomethyl)-2-nitropropane-1,3-diol (AZONITRO, 3) [11]

In a 250 mL round-bottom flask the ketal, (Compound **2a**) (8.61 g, 45 mmol) was dissolved in pyridine (18 mL) and cooled to -15^{o}C. To the stirred solution, tosyl chloride (9.173 g, 48 mol), dissolved in 13.5 mL dioxane, was added dropwise and allowed to stir overnight at room temperature. The mixture was poured over sodium bicarbonate (2.025 g) in 90 g of ice water. The white precipitate was isolated by vacuum filtration yielding 2,2-dimethyl-5-nitro-1,3-dioxan-5-yl 4-methylbenzenesulfonate (Compound **3a**) 11.31 g (72% yield).

In a 250 mL round-bottom flask Compound **3a** (9.22 g, 26.7 mmol) was dissolved in 75 mL of dimethylformamide; sodium azide (8.80 g, 135 mol) was added, and the mixture refluxed at 60°C for 24 hours. The slurry was poured over 135 g of ice and extracted with four aliquots of ethyl acetate (150 mL). The extracts were combined, washed with 4 portions of deionized water (150 mL), and dried over sodium sulfate. The sodium sulfate was removed by vacuum filtration; and the ethyl acetate, by rotary evaporation. Xylenes (50 mL) were added to create an azeotrope for the excess DMF;

they were removed together by rotary evaporation. Crystals of 5-(azidomethyl)-2,2-dimethyl-5-nitro-1,3-dioxane (Compound **3b**) were removed from the round bottom to yield 5.1 g (88%).

In a 250 mL round-bottom flask, Compound **3b** (4.9 g, 22.7 mmol) was combined with methanol (80mL) and 12M HCl (8mL) and refluxed at 60°C for 24 h. At room temperature, HCl and methanol were removed by rotary evaporation to produce dark amber oil, 2-(azidomethyl)-2-nitropropane-1,3-diol, Compound **3** with quantitative yield (4.2 g) (Figure 2.4).

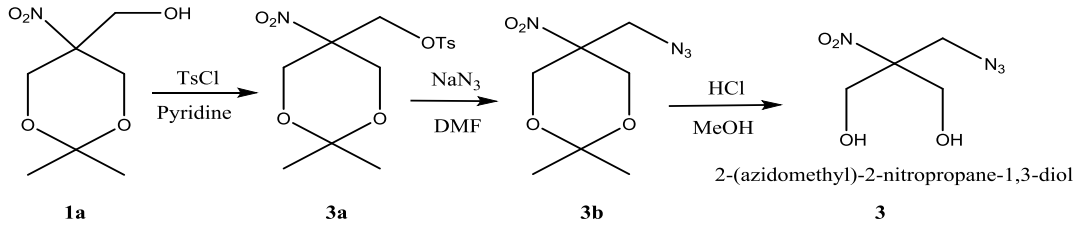

Figure 2.4. Synthesis of 2-(Azidomethyl)-2-nitropropane-1,3-diol (AZONITRO, **3**)

2,2-Bis(Azidomethyl)propane-1,3-diol (BAMP, 4) [12-14]

In a 250 mL round bottom flask, 2,2-bis(bromomethyl)propane-1,3-diol (Compound **4a**) (2.8 g, 10.7 mmol) and sodium azide (1.74 g, 28.8 mmol) were dissolved in 20 mL DMSO. The solution was heated at 100 °C for 48 h. Then proportional amounts of water and brine were added (15 mL). The solution was extracted with three 20 mL portions of ethyl acetate. The ethyl acetate solution was dried with sodium sulfate, filtered, and remaining liquid removed by rotary evaporation yielding 1.90 g (95%) of light yellow oil Compound **4** (Figure 2.5).

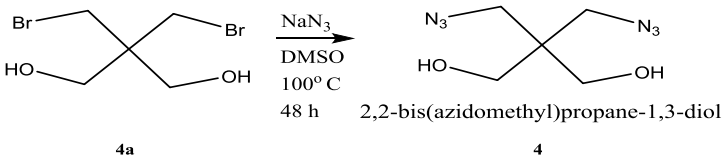

Figure 2.5. Synthesis of 2,2-Bis(Azidomethyl)propane-1,3-diol (BAMP, **4**)

2,2-Dinitro-1,3-propanediol (DNPD, 5) [13-16]

In a 500 mL round-bottom flask, 4.50 g of sodium hydroxide was dissolved in 200 mL of water. The ketal, Compound **1a**, (10.15 g, 53 mmol) was added and stirred until dissolved. A solution of potassium ferricyanide (1.87 g) and sodium nitrite (14.7 g) in 30 mL of distilled water was added to the flask. The flask was put into an ice bath, and solid sodium persulfate (13.36 g) was added in portions while keeping the temperature below 30°C. The turbid solution was stirred for an additional 2 hours before the precipitate was collected by vacuum filtration, washed with cold distilled water, and air dried to yield 8.07 g of 2,2-dimethyl-5,5-dinitro-1,3-dioxane (86%) (Compound **5a**), a light cream colored product with a melting point of 53-54°C.

To prepare Compound **5**, in a 250 mL round-bottom flask, Compound **5a** (8.07 g 39 mmol) was dissolved in 100 mL methanol and 14 mL of 12M HCl and heated at 60°C in an oil bath overnight. At room temperature, the HCl and methanol were removed by rotary evaporation; and the solid, dried to yield Compound **5,** 5.20 g (80%) with a melting point of 135°C (Figure 2.6).

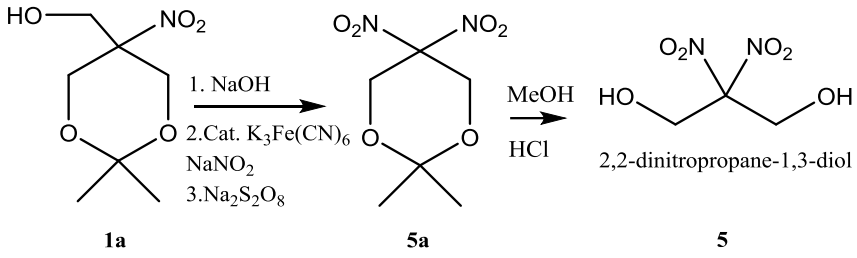

Figure 2.6. Synthesis of 2,2-Dinitro-1,3-propanediol (DNPD, **5**)

Polyurethane Foams

General Procedure of (TEOA-TDI) polyurethane foam synthesis

Part A consisted of toluene diiosocyanate (TDI) (1 mL, 7.0 mmol) in 500 µL pentane to which 1 wt% DOW surfactant TRITON^{TM} GR-7M. The two miscible liquids were stirred in a centrifuge tube. **Part B** consisted of triethanolamine (TEOA, 500 µL, 3.0 mmol, 80% wt in water) and the catalyst, triethylamine (TEA, 250 µL, 1.8 mmol). Increasing concentration of the catalyst increased the rate of foam formation; a near instantaneous reaction was desired [17-18]. If applicable the specially synthesized monomer, and a small amount of acetone was used to adjust viscosity. For the standard TEOA-TDI synthesis, **Part B** was added to **Part A**, for synthesis involving the special monomers, **Part A** was added to **Part B'**. The reaction took 5 seconds, increasing in temperature as it cured to form the standard polyurethane (TEOA-TDI); it exhibited significant expansion (9X) and hardening to withstand stimulation with a glass stir rod. The exothermic cure of polyurethane foams can reach temperatures at high as 140-170 °C which result in 'scorching' of the polymer. Scorching weakens the urethane linkages so that they no longer withstand the mechanical stress associated with high solids loading [6]. The TEOA-TDI foam was white in color with no visible scorching (Figure 2.7). This synthetic method was altered using special energetic monomers, starting at 50:50 mole ratios, and varying until foam had a desirable structure and expansion factor.

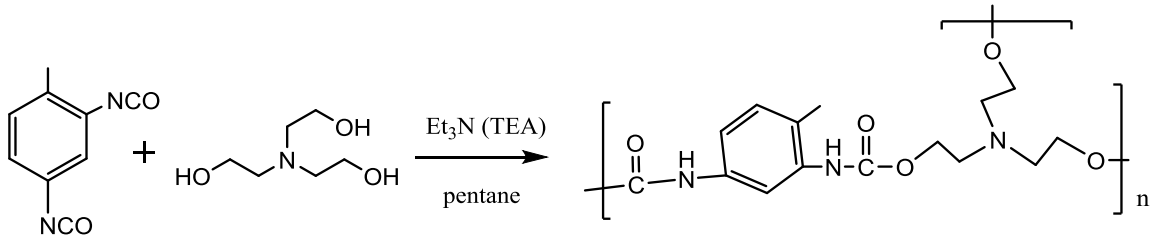

Figure 2.7. Synthesis of (TEOA-TDI) foam

Foam of Compound **1 (TMNM(1)/TEOA-TDI)**

A solution was formed (2.6 mL) from TMNM **1** (0.75 g, 5 mmol), and TEOA (1.12 g ,7.5 mmol), and 1 mL of acetone. An aliquot of this solution (500 µL) containing 1.0 mmol TMNM, and 1.5 mmol TEOA was added to TEA (250 µL, 1.8 mmol) and mixed in a 50 mL centrifuge tube; this was **Part B'**. **Part A** (the isocyanate solution) was added to **Part B'**; they were initially immiscible, but after swirling the mixture for about 4 seconds resulted in an increase in temperature and miscibility. At 10 seconds the reaction began to bubble, and the resulting foam expanded to 10X the original volume. This foam was yellow with no visible scorching and more crystalline in structure than the TEOA-TDI foam. It withstood stimulation with a glass stir rod (Figure 2.8).

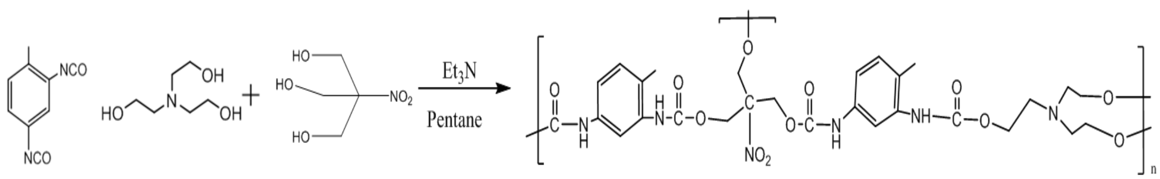

Figure 2.8. Synthesis of (TMNM(**1**)/TEOA-TDI) foam assuming 1:1 mol Polyol

Foam of Compound **2 (TETRA(2)/TEOA-TDI)**

A dark red stock solution (2.5 mL) was formed by adding TETRA **2** (1 g, 4.2 mmol) and TEOA (1 g, 6.7 mmol) to 500 µL acetone. **Part B'** was prepared in a 50 mL centrifuge tube by adding TEA (100µL, 1.0 mmol) to an aliquot (650 µL) of the red solution (1.0 mmol TETRA and 1.7 mmol TEOA). **Part A** (the TDI solution) was added to **Part B'**; an instantaneous reaction began; and the foam expanded 10X the original volume. The resulting foam was not stiff enough to withstand stimulation with a glass stir rod (Figure 2.9). It was easily powdered with mortar and pestle. It was dark red in color, and, despite several procedure changes, exhibited some visible scorching in the middle. Starting at 50:50 mole ratio of TETRA to TEOA, the amount of TETRA **2** was reduced

until the TETRA to TEOA ratio was 0.4. Even at this low ratio, scorching was observed in the center of the polymer mass. Lowering catalyst to 50 µL didn't eliminate scorching.

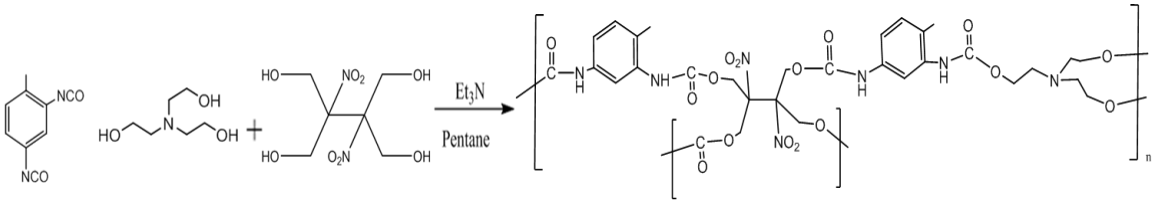

Figure 2.9. Synthesis of (TETRA(**2**)/TEOA-TDI) **f**oam assuming 1:1 mol Polyol

Foam of Compound **3 (AZONITRO(3)/TEOA-TDI)**

One gram each of AZONITRO **3** (5.7 mmol) and TEOA (6.7 mmol) were mixed in acetone (500 µL) to form 2.5 mL of a viscous, orange solution. In a 50 mL centrifuge tube an aliquot (1 mL) of the orange solution [AZONITRO (2.2 mmol) and TEOA (2.7 mmol)] was mixed with TEA catalyst (100 µL, 1.0 mmol) to create **Part B'**. **Part A** was added to **Part B'**; in 10 seconds the reaction was complete, and the foam had expanded 9 times the original volume. This orange foam showed no scorching and could withstand stimulation with a glass stir rod (Figure 2.10).

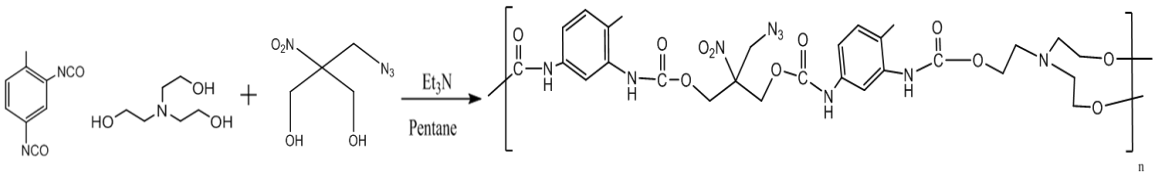

Figure 2.10. Synthesis of (AZONITRO(**3**)/TEOA-TDI) Foam assuming 1:1 mol Polyol

Foam of Compound **4 (BAMP(4)/TEOA-TDI)**

A transparent yellow solution (1.5 mL) was formed by adding BAMP **4 (**1 g, 5.4 mmol) and TEOA (0.5 g, 3.4 mmol) to 500 µL of acetone. A 1 mL aliquot of this solution, containing BAMP (2.7 mmol) and TEOA (1.7 mmol) was mixed with TEA (150 µL, 1.1 mmol) in a 50 mL centrifuge tube to make up **Part B'**. **Part A** was added to **Part**

B', and the foam formed and expanded 7 fold in about 6 seconds. This white foam showed no visible scorching and withstood stimulation with a glass stir rod (Figure 2.11).

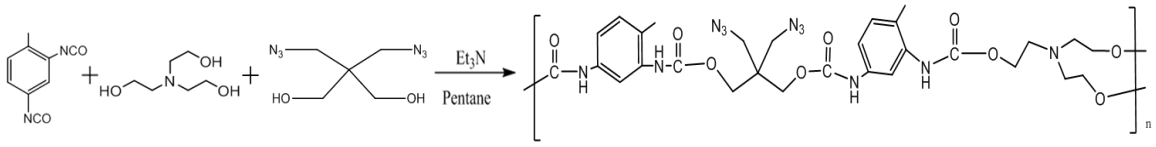

Figure 2.11. Synthesis of (BAMP(**4**)/TEOA-TDI) Foam assuming 1:1 mol Polyol

Foam of Compound **5 (DNPD(5)/TEOA-TDI)**

Countless attempts to make a foam using as little DNPD (0.10 g, 0.6 mmol) to TEOA (0.15g, 1.0 mmol) and reducing catalyst to 50 µL resulted in a full scorching of the foam with concomitant orange fumes.

Foams with Pyrotechnic

To examine how significant amounts of solids loading affected polymer formation or expansion, the following experiment was performed. **Part A** was placed in a centrifuge tube and stirred. **Part B,** which consisted of TEOA and TEA**,** was added to **Part A**. Immediately after the reaction began, discernable by yellow coloration, and before bubbling commenced, the pyrotechnic was added, an amount equivalent to 73% solids loading. The pyrotechnic formulation was a 90/10 $Ca(IO_3)_2$/Al mixture, 73% solids loading is equivalent to 4.84 g pyrotechnic per 1.80g foam. The reaction mixture was stirred once before it began to expand; the reaction was complete in 20 seconds or less. The product was porous, grey in color, and exhibited similar expansion (8X) to the foam without solids.

Scanning Electron Microscope (SEM)/ Energy Dispersive Spectroscopy (EDS)

Pyrotechnic-loaded polyurethane foam samples were dried in a vacuum oven and transported in falcon tubes. Small slivers were cut with razor blade from the top and bottom of the expanded pyrotechnic-loaded foam. Samples were placed on the sample holder examined under low vacuum (25 Pa) in backscatter mode at a voltage of 20 kV.

Powdered Foams with Pyrotechnic

For calorimetry, foams were ground in a coffee grinder and sieved to particle sizes of 150-300 µm. They were mixed in a Resodyn™ Acoustic Mixer with pyrotechnic.

Bomb Calorimetry/UV-VIS

Bomb Calorimetry was performed using a Parr 6200 Isoperibol Bomb Calorimeter. The calorimeter was calibrated (10 trials) with benzoic acid and 2.07 MPa oxygen (ΔU_c = 26.4 kJ/g). The samples were loaded and ignited in O_2 (2.07 MPa).

When molecular iodine (I_2) was produced in the bomb calorimetric experiments, it was quantified using an ultraviolet-visible (UV-Vis) spectrometer (Agilent 8453), 190 to 1100 nm, resolution 1 nm, 0.5 s integration time. Iodine was extracted from the bomb with 100 mL of an aqueous 0.5 M potassium iodide (KI) solution. The solution had excess I^- which solubilized I_2 and transformed it to I^{3-} (λ=353 nm) [19]. An example of a calibration curve for iodine quantification is shown in Figure 2.12.

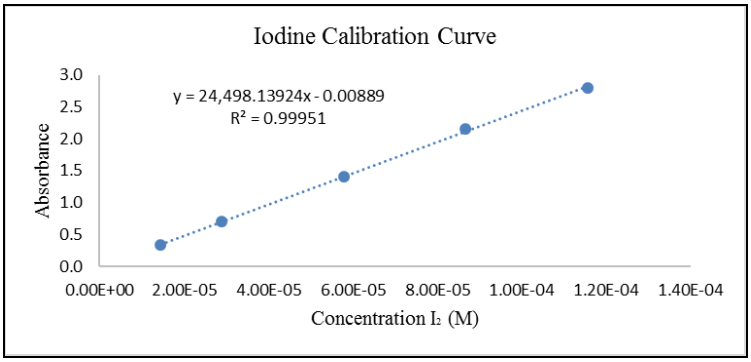

Figure 2.12. Example UV-Vis calibration curve for I_2 quantification

RESULTS AND DISCUSSION

Monomers

Characterization

FTIR

In Figure 2.13, the FTIR of each monomer used is shown. At around 3200 cm^{-1} the OH stretch is visible and broad for all cases. In spectra 1,2,3 and 5, the stretch for NO_2 are seen at 1560-1510 cm^{-1}. In spectra 3 and 4, the N_3 stretch is sharp at 2100 cm^{-1}.

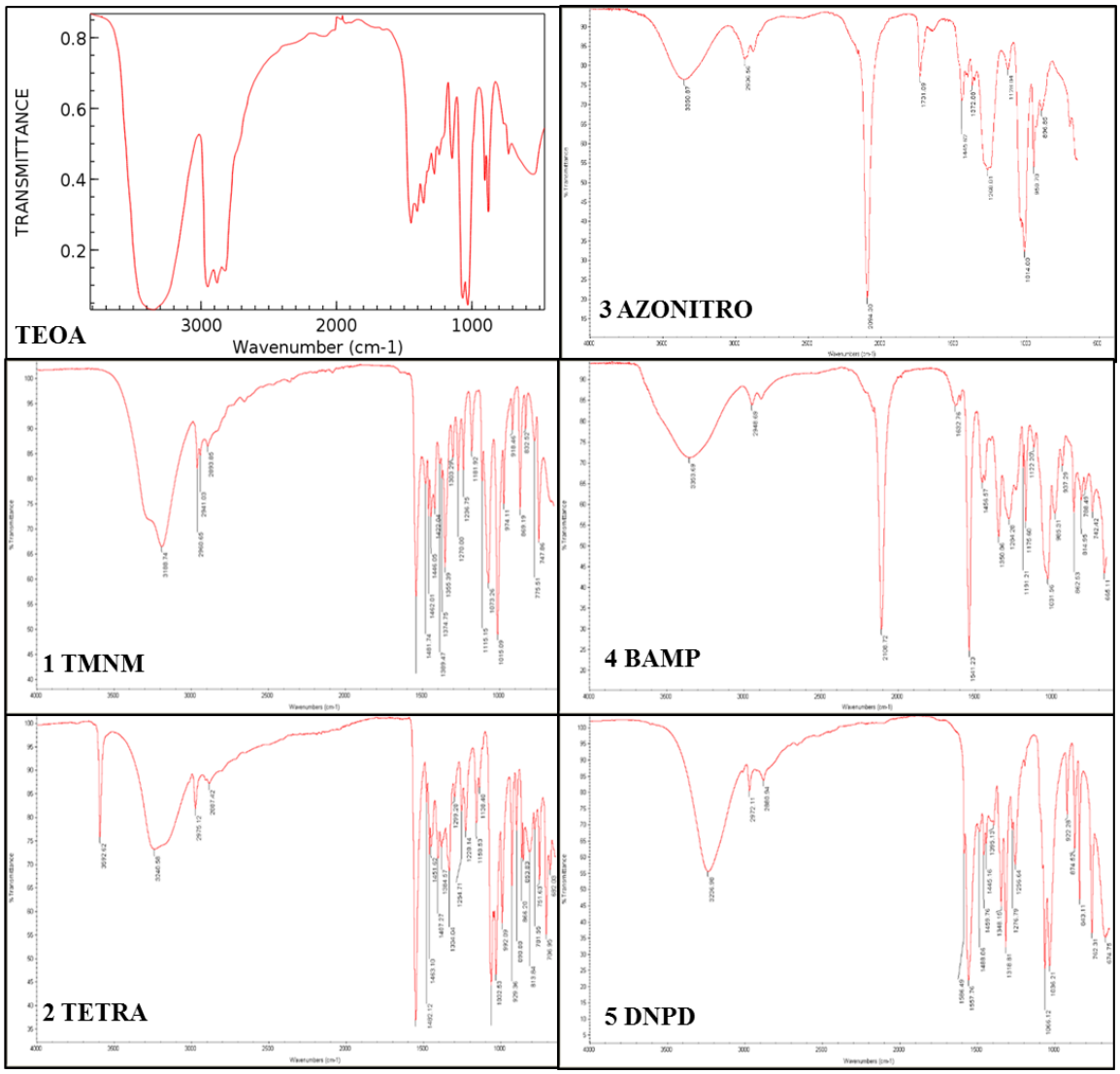

Figure 2.13. IR Spectra of TEOA (provided by NIST Chemistry WebBook), TMNM (**1**), TETRA (**2**), AZONITRO (**3**), BAMP (**4**), and DNPD (**5**)

LCMS

In order to confirm the synthesis of the monomers, LCMS was performed. Figure 2.14 shows the results from the mass spectrometer. TETRA (**2**) formed a fragment [TETRA - OH] with an exact mass of 209.0415 AMU, and a chloride adduct [TETRA + Cl^-] with an exact mass of 275.0281 AMU. In the case of the AZONITRO compound (**3**), there was only one peak to verify identification, a chloride adduct [AZONITRO + Cl^-] with an exact mass of 211.0237 AMU. BAMP (**4**) formed two adducts, a chloride adduct [BAMP + Cl^-] with an exact mass of 211.0560 AMU, and a formate adduct [BAMO + $CHOO^-$] with an exact mass of 231.0848 AMU. DNPD (**5**) formed a similar fragment to TETRA [DNPD - OH] with an exact mass of 135.0048 AMU, and a chloride adduct [DNPD + Cl^-] with an exact mass of 200.9917 AMU.

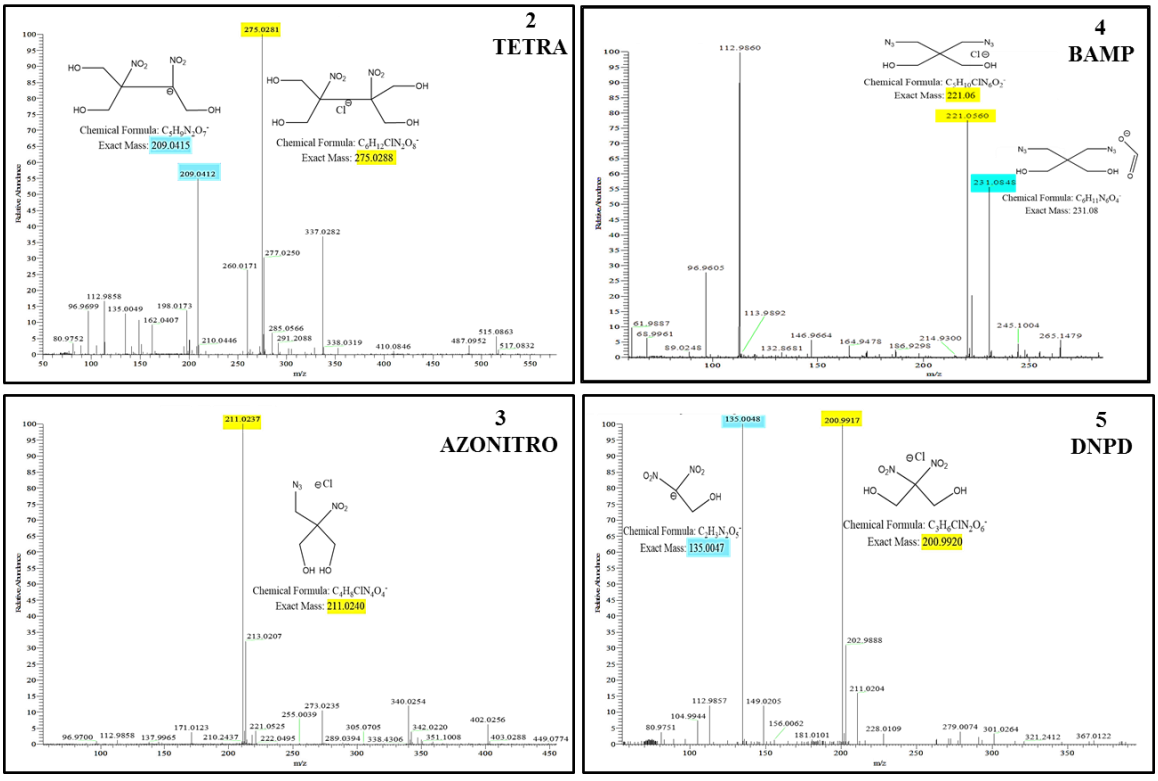

Figure 2.14. LCMS Confirmation TETRA (**2**), AZONITRO (**3**), BAMP (**4**)**,** & DNPD (**5**)

DSC

In Figure 2.15, DSC traces of the monomers used are shown at 20 °C min^{-1}. TEOA, the non-energetic monomer has an endothermic decomposition at 198 °C. All the energetic synthesized monomers (1-5) have exotherms in the 200-260 °C region. The three crystalline energetic monomers show endotherms at their melting points (1, 2 and 5). The two liquid energetic monomers, (3 and 4), have only a single exotherm.

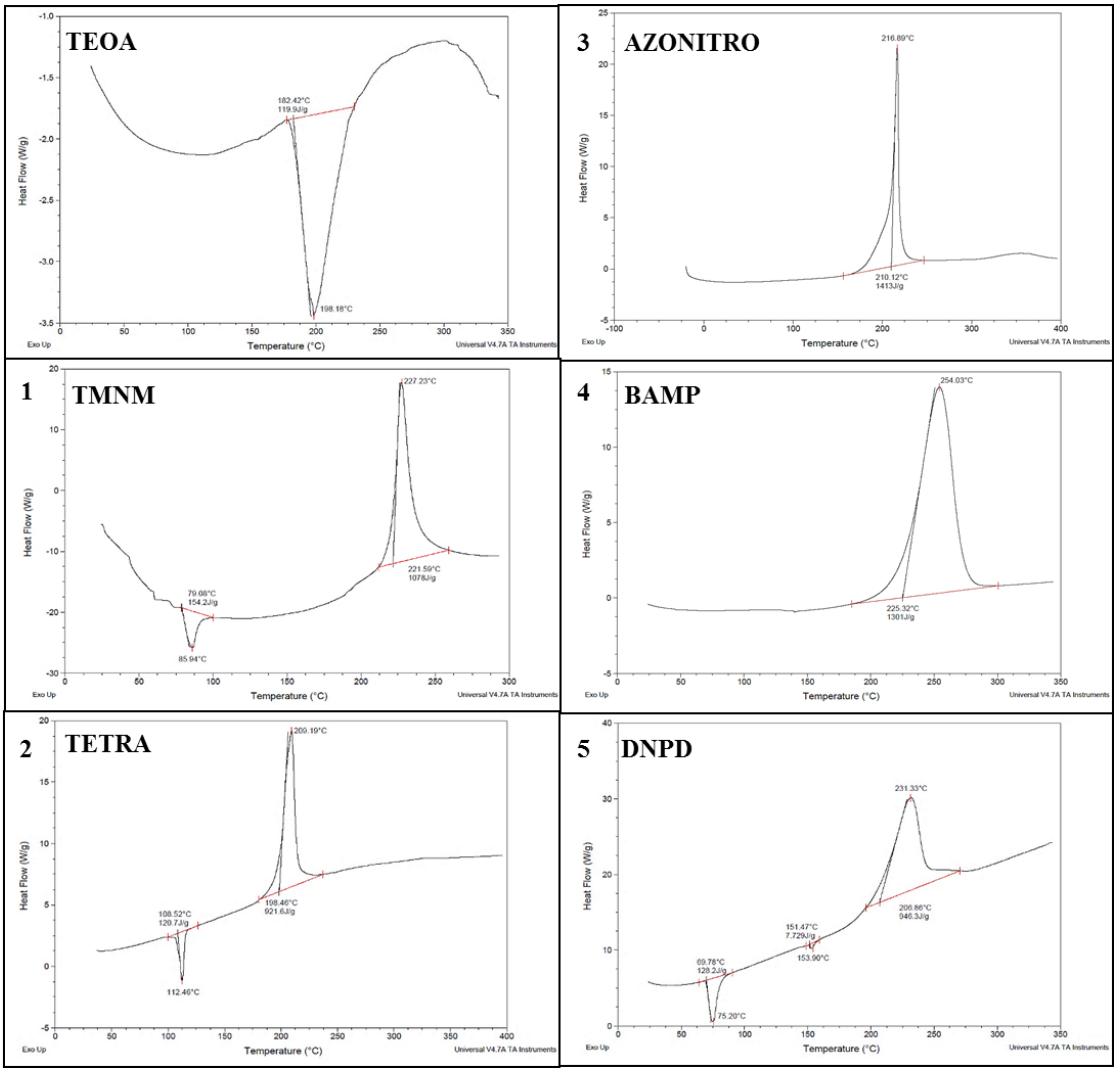

Figure 2.15. DSC Traces TEOA, TMNM (**1**), TETRA (**2**), AZONITRO (**3**), BAMP (**4**), & DNPD (**5**)

Polyurethane foams

Characterization

FTIR

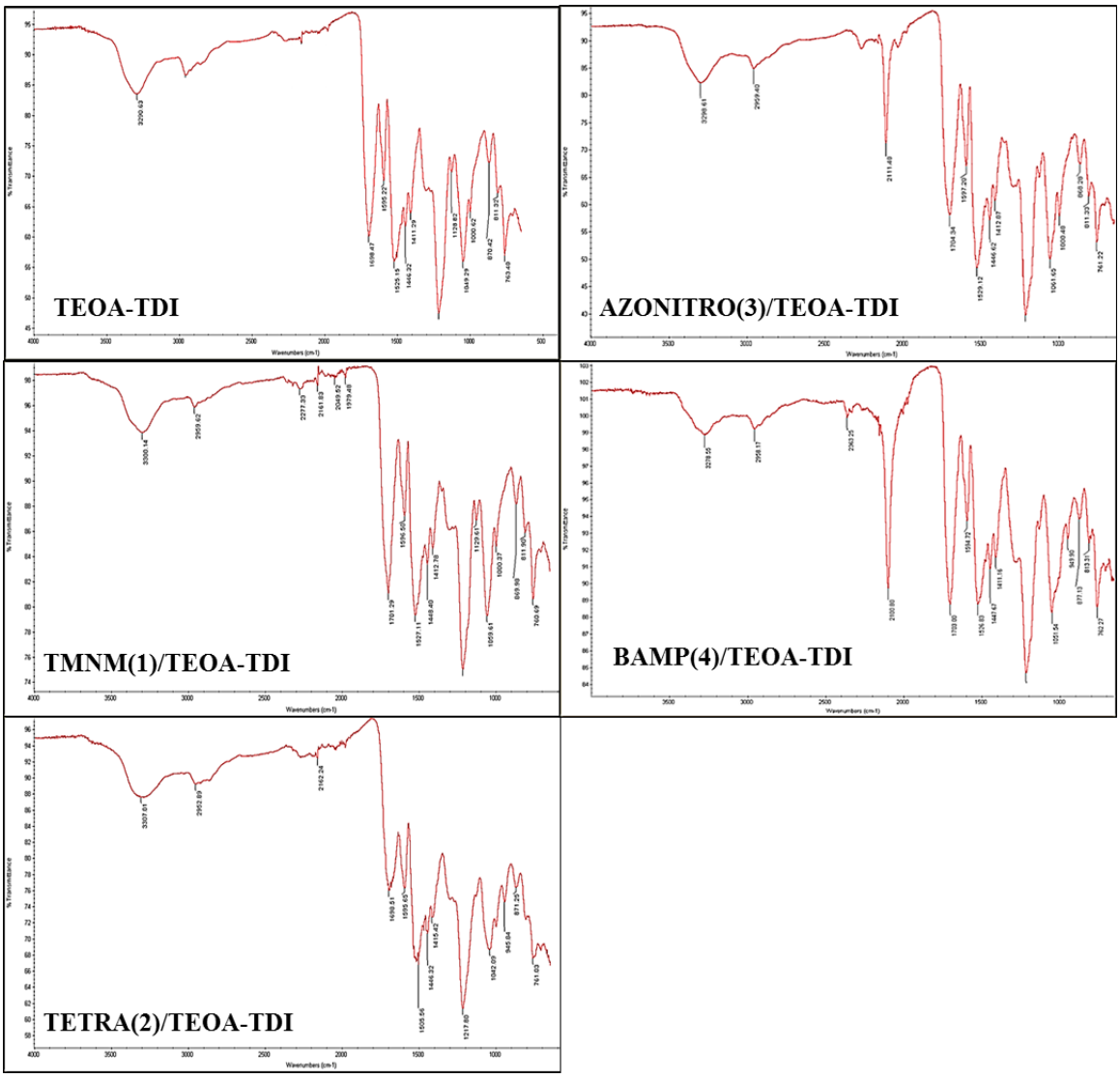

Figure 2.16. IR Spectra of Polyurethane Foams TEOA-TDI, TMNM(**1**)/TEOA-TDI, TETRA(**2**)/TEOA-TDI, AZONITRO(**3**)/TEOA-TDI, & BAMP(**4**)/TEOA-TDI

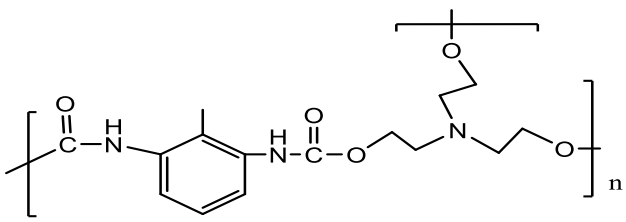

Figure 2.17. Schematic of TEOA-TDI foam

The FTIR characteristics are shown in Figure 2.16. In Figure 2.17, for the standard foam (TEOA-TDI) the following stretches are observed: ATR $\tilde{\nu}$= 3290 cm^{-1} is the N-H valence vibration, 1700 cm^{-1} is the valence vibration of the C=O group (amide I), 1525 cm^{-1} is the amide II vibration (N-H bending), and 1220 cm^{-1} is the asymmetric C-O bending vibration. Foams TMNM(1)/TEOA-TDI and TETRA(2)/TEOA-TDI, only have (NO_2) functionality, which literature suggests, overlaps with the C-O asymmetric vibration at around 1520 cm^{-1} (can be seen anywhere between 1500-1600 cm^{-1}) [14]. In Figure 2.16, AZONITRO(3)/TEOA-TDI and BAMP(4)/TEOA-TDI the quintessential (N_3) vibration can be seen at around 2100 cm^{-1}.

Thermal Properties

SDT

Thermal traces of the five polyurethane foams run on TGA and DSC simultaneously show clear, two-step weight loss, the first centered around 250 °C and the second around 420 °C Figure 2.18. In the standard polyurethane, the first weight loss is endothermic, whereas in the polymers modified with the energetic monomers [TMNM(**1**)/TEOA-TDI, AZONITRO(**3**)/TEOA-TDI, and BAMP(**4**)/TEOA-TDI] this weight loss is exothermic. Above 350 °C, all the polyurethanes exhibit endothermic weight loss, until by 450 °C no polymer remains. These traces are interpreted as initial partial decomposition of the monomer, followed by complete pyrolysis of the organic species.

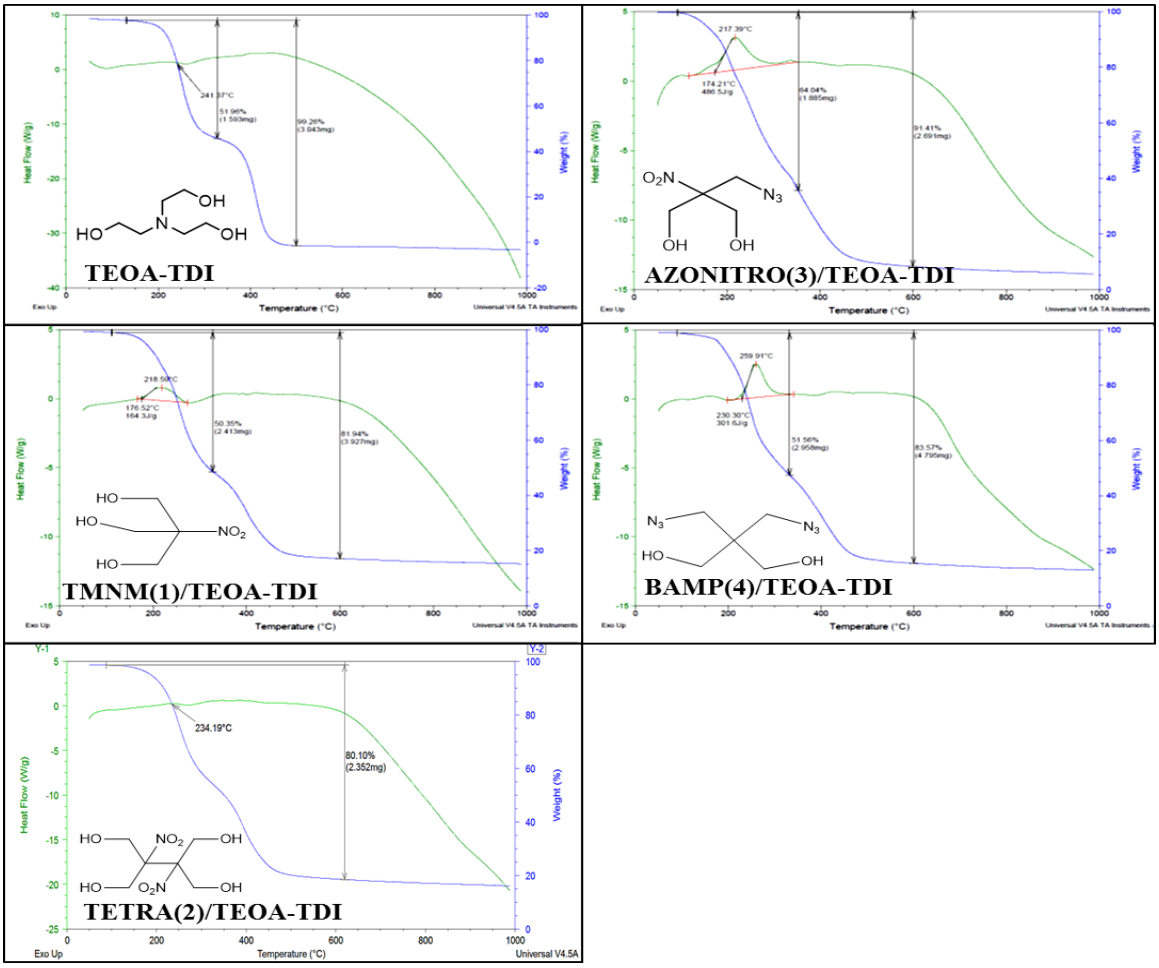

Figure 2.18. SDT of Polyurethane Foams TEOA-TDI, TMNM(**1**)/TEOA-TDI, TETRA(**2**)/TEOA-TDI, AZONITRO(**3**)/TEOA-TDI, & BAMP(**4**)/TEOA-TDI

In Table 2.1, the components for the synthetic routes for each foam type are laid out along with foam characteristics-- expansion factor, heat of combustion (ΔU_c), and heat of decomposition (ΔH). Expansion factor was calculated based on the ratio of the milliliters of liquid components, to the milliliters of the expanded foam, for example: 5 mL/45 mL = 9X (Figure 2.19). The heat of combustion, ΔU_c, was experimentally determined using bomb calorimetry. Heat of decomposition, ΔH, values were experimentally determined using SDT.

Figure 2.19 Expansion of foams, from left to right: TEOA-TDI, TMNM(**1**)/TEOA-TDI, TETRA(**2**)/TEOA-TDI, AZONITRO(**3**)/TEOA-TDI, BAMP(**4**)/TEOA-TDI

Table 2.1. Components of polyurethanes prepared with special monomers

TEOA-TDI Foam									
Part A			Part B				Expansion	ΔUc (kJ/g)	ΔH (J/g)
Compostion	mg	mmol	Composition	mg	mmol				
TDI	1214	7.0	**TEOA**	560	3.0				
Pentane	313	4.3	**TEA**	181.5	1.8		9X	**23.5**	**0**
mmol NCO			mmol OH						
13.9			9.0						
TMNM(1)/TEOA-TDI Foam									
Part A			**Part B**				Expansion	ΔUc (kJ/g)	ΔH (J/g)
Compostion	mg	mmol	Composition	mg	mmol	ratio 1 to TEOA			
TDI	1214	7.0	**TEOA/TMNM**	225/150	1/1.5	0.67			
Pentane	313	4.3	**TEA**	181.5	1.8		10X	**19.1**	**165**
mmol NCO			mmol OH						
13.9			7.5						
TETRA(2)/TEOA-TDI Foam									
Part A			**Part B**				Expansion	ΔUc (kJ/g)	ΔH (J/g)
Compostion	mg	mmol	Composition	mg	mmol	ratio 2 to TEOA			
TDI	1214	7.0	**TEOA/TETRA**	250/250	1.7/1	0.59			
Pentane	313	4.3	**TEA**	72.6	1.0		10X	**25.9**	**0**
mmol NCO			mmol OH						
13.9			9.1						
AZONITRO(3)/TEOA-TDI Foam									
Part A			**Part B**				Expansion	ΔUc (kJ/g)	ΔH (J/g)
Compostion	mg	mmol	Composition	mg	mmol	ratio 3 to TEOA			
TDI	1214	7.0	**TEOA/AZO**	400/400	2.7/2.2	0.81			
Pentane	313	4.3	**TEA**	72.6	1.0		9X	**22.6**	**487**
mmol NCO			mmol OH						
13.9			12.5						
BAMP(4)/TEOA-TDI Foam									
Part A			**Part B**				Expansion	ΔUc (kJ/g)	ΔH (J/g)
Compostion	mg	mmol	Composition	mg	mmol	ratio 4 to TEOA			
TDI	1214	7.0	**TEOA/BAMP**	250/500	1.7/2.7	1.6			
Pentane	156.5	2.2	**TEA**	108.9	1.1		7X	**22.5**	**300**
mmol NCO			mmol OH						
13.9			10.5						

Pyrotechnic Foams

The standard foam TEOA-TDI was used to test how much pyrotechnic powder and how uniformly this powder could be introduced to the foam. The pyrotechnic mixture was added to TEOA-TDI in amounts ranging from 30 wt% to 80 wt%. It was determined that up to 73 wt% powdered pyrotechnic could be added without significantly compromising expansion (expansion was 8 fold rather than 9). To determine the uniformity of distribution of the pyrotechnic, a top and bottom sliver of the pyrotechnic-loaded TEOA-TDI foam was examined by SEM/EDS. Distribution was less uniform than desirable. The micrographs in Figure 2.20 show more pyrotechnic in the bottom slice than the top.

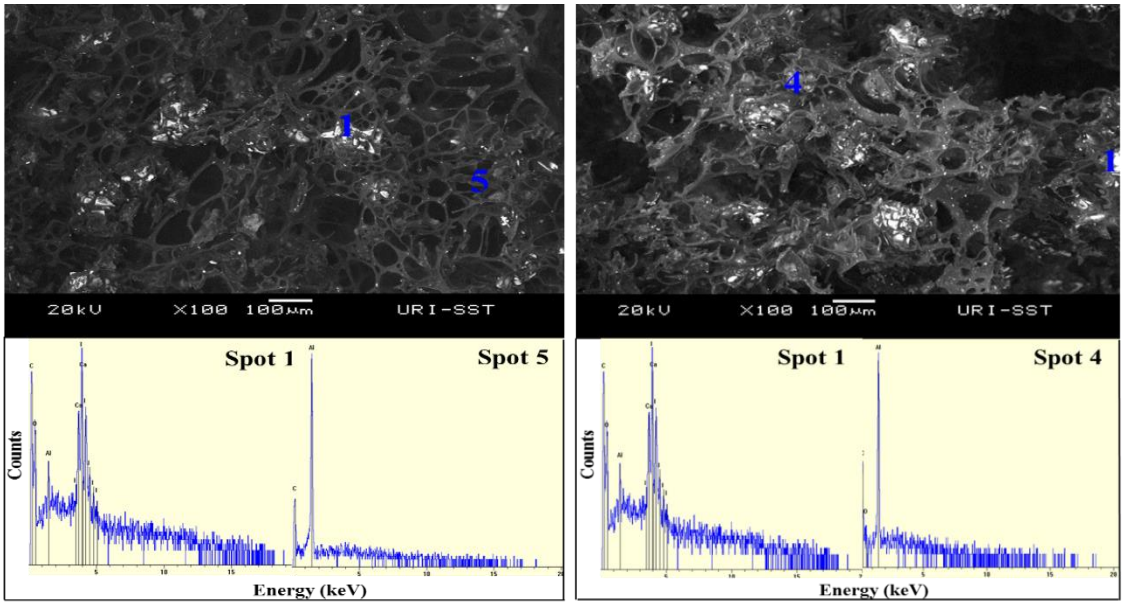

Figure 2.20. SEM micrographs TEOA-TDI foam, 70% solids loading 90/10 $Ca(IO_3)_2$/Al EDS foam top (left)(Spot 1 Ca & I; Spot 5, Al); bottom (right)(Spot 1 Ca & I; Spot 4, Al)

Without the presence of foam, the $Ca(IO_3)_2$/Al ratio which would readily burn was 75/25. With added organic, a 90/10 ratio gave optimum performance (Fig. 2.21)

Iodine production %I_2/mix gram	90/10 $Ca(IO_3)_2$ +30 % FOAM	95/5 $Ca(IO_3)_2$ +30 % FOAM	75/25 $Ca(IO_3)_2$ +30 % FOAM
Heat (kJ/g)	34	30	29
	9.04	8.32	11.69

Figure 2.21. Open burn of TEOA-TDI foam compared with bomb calorimetry values for molecular iodine and heat production

With the exception of TETRA(**2**)/TEOA-TDI, all the polymers shown in Table 2.1 were mixed with 70 wt% pyrotechnic mixture of 90/10 $Ca(IO_3)_2$/Al and the heats of combustion and iodine production determined by bomb calorimetry. TETRA(**2**)/TEOA-TDI was not chosen for further study because its charring suggested that mixing with a pyrotechnic might result in hazardous, unexpected ignition. To overcome the lack of uniform distribution of the pyrotechnic in the foams, for calorimetry only, the foams were powderized, and 70 wt% of the pyrotechnic (90/10 $Ca(IO_3)_2$/Al) was mixed in (Table 2.2). SDT of the pyrotechnic-loaded energetic and standard foams (Figure 2.22) show the pyrotechnic mixture releases heat earlier and over a longer range than without an organic matrix.

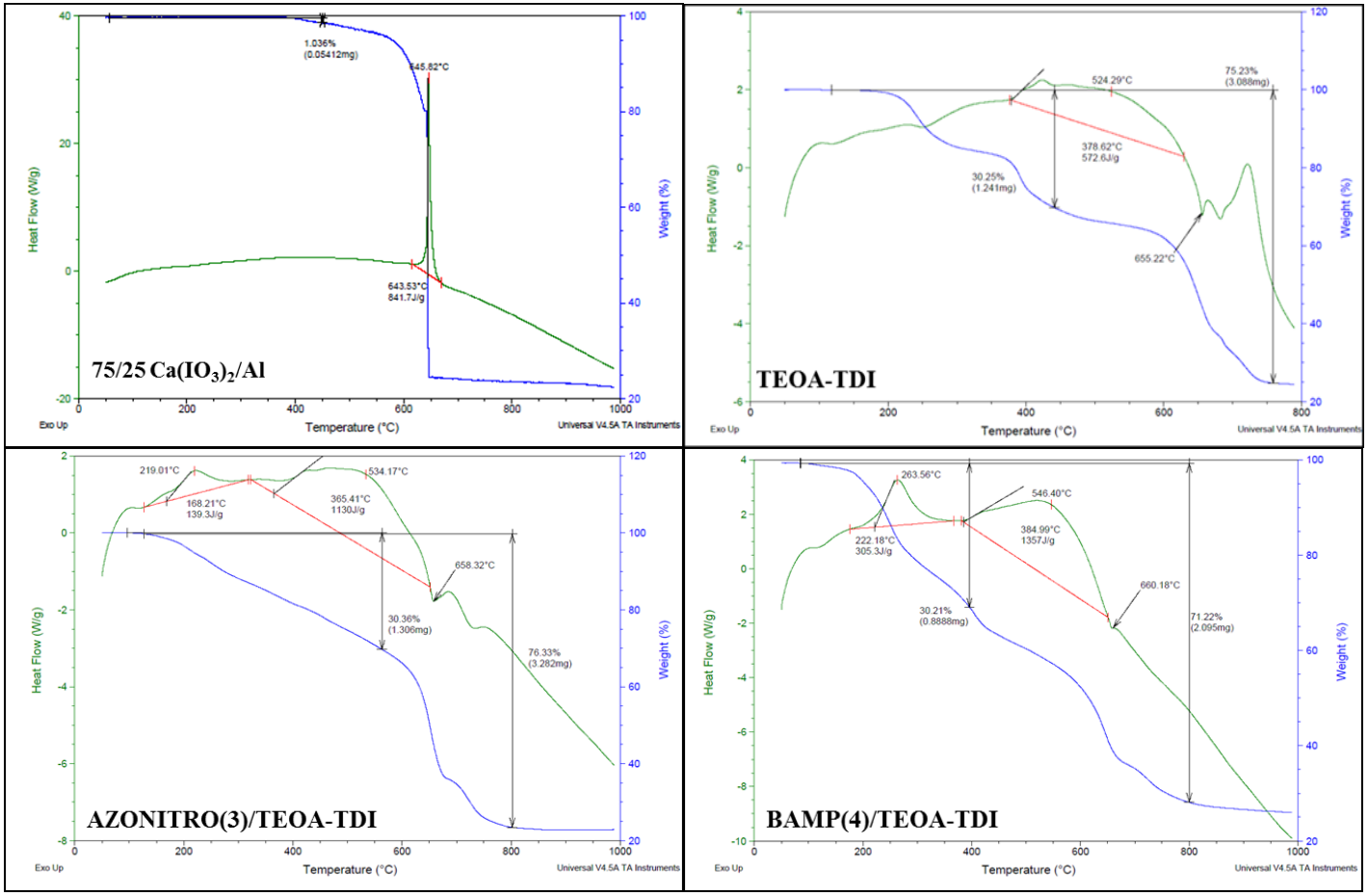

Figure 2.22 SDT of Ca(IO3)2/Al alone (top left) versus polyurethane foams w added pyrotechnic (90/10 Ca(IO3)2 + 30% foam) TEOA-TDI foam, TEOA/AZONITRO(3)-TDI foam, TEOA/BAMP(4)-TDI foam

Table 2.2. Bomb calorimetric results for pyrotechnic-loaded foams under oxygen

Pyrotechnic-loaded Foam	Heat Output (kJ/g)	std dev	% Iodine (I_2 formed to pyro mass)	std dev
90/10 Ca(IO3)2 /Al +30% TEOA-TDI Foam	9.04	0.38	34.0	1.84
90:10 Ca(IO3)2/Al/+30% TMNM(1)/TEOA-TDI Foam	8.72	0.15	32.4	1.81
90:10 Ca(IO3)2/Al/+30% AZONITRO(3)/TEOA-TDI Foam	7.52	0.66	36.7	0.80
90:10 Ca(IO3)2/Al/+30% BAMP(4)/TEOA-TDI Foam	8.99	0.21	36.8	1.21

Within standard deviation the pyrotechnic-loaded energetic foams do not outperform the standard foam. This was not the case for the polymers when no pyrotechnic was present (Table 2.1). Apparently, the boost in energy and oxygen production provided by the pyrotechnic (70 wt% loading) overwhelms any addition boost available from the energetic monomer which makes up less than 10 wt% of the overall formulation.

CONCLUSIONS

This study sought to improve the energy output of polyurethane/pyrotechnic formulations by replacing part of the polyol TEOA with polyols containing nitro and/or azide groups. Monomers containing one or two of these functional groups were synthesized, but it was found that the presence of two nitro groups in the polyol, as in Compounds **2** and **5**, resulted in a material so energetic that when combined with TDI, the polyurethane could not be produced without "scorching." It should be noted that polyurethane resins have been made from compounds **4** and **5**, but in that report polymerization was allowed to progress slowly (overnight) [14]. In contrast, the diazo group, one nitro group, and one azo/one nitro were successfully inserted into a polyurethane. We believe TMNM **1** and AZONITRO **3** polyurethanes are reported here for the first time.

It was found that a pyrotechnic powder could be mixed with the polyurethane foams at levels up 73% solids with little negative impact on the foam expansion; it was only reduced from 9 to 8 fold. Furthermore, the pyrotechnic added could contain less aluminum since fuel was supplied by the polyurethane. Whereas at least 25% aluminum was required to produce ignition in a $Ca(IO_3)_2$ powder, in the presence any of the polyurethane foams the oxidizer/aluminum ratio could be raised to 90/10 and still be readily ignited. Reduction of aluminum resulted in increased output of molecular iodine.

REFERENCES

1. H. Fairhead, B. Setlow, P. Setlow, Prevention of DNA Damage to Spores and In Vitro by Small, Acid-Soluble Proteins from Bacillus Species. *J. Bacteriology*, **1993**, 175 (5), 1367-1374.

2. B.R. Clark, M.L. Pantoya, The aluminum and iodine pentoxide reaction for the destruction of spore forming bacteria, *Phys. Chem. Chem. Phys.* **2010**, 12 (39), 12653-12657.

3. R. Tennen, B. Setlow, K.L. Davis, C.A. Loshon, P. Setlow, Mechanisms of killing spores of Bacillus subtilis by iodine, glutaraldehyde, and nitrous acid. *J. Appl. Microbiol.*, **2000**, 89, 330-338.

4. S.P. Gorman, E.M. Scott, E.P. Hutchinson, Effects of aqueous and alcoholic providone-iodine on spores of Bacillus subtilis. *J. Appl. Bacteriol.*, **1985**, 59 (1), 99-105.

5. Oxley, J.C..; Smith, J.L.; Porter, M.M.; Yekel, M.J.; Canaria, J.A. "Potential Biocides" Iodine-Producing Pyrotechnics" *Propellants Explos. Pyrotech*., submitted.

6. Bailey, F.E. Jr. Flexible Polyurethane Foams. In *Handbook of Polymeric Foams and Foam Technology*; Klempner, D; Frisch, K.C.; Hanser, Munich, 1991; p 53/68.

7. McGuire, R.R.; Cochoy, R. E.; Shackelford, S. A.; Process for preparation of energetic plasticizers. US 4424398, January 3, **1984**.

8. Provatas, A.; *Energetic Polymers and Plasticisers for explosive formulations- A review of recent advances*. DSTO: Melbourne, 2000.

9. Ghee Ang, H. and Pisharath, S. Energetic Polymers: binders and plasticizers for enhancing performance; Wiley: Wienhiem, **2012**, 1-18.

10. Oxley, J. C.; Smith, J. L., Brady IV, J. E.; Brown, A. C.; Characterization and Analysis of Tetranitrate Esters. *Propellants Explos. Pyrotech*. **2012**, *37*, 24-39.

11. Schulze, M.C.; Chavez, D. E.; Synthesis and characterization of energetic plasticizer AMDNNM. *J. Energ. Mater.*, **2016**. 34 (2), 129-137.

12. Diaz, D.D.; Punna, Sreenivas; Holzer, P; Mcpherson, A. K.; Sharpless, B.; Fokin, V.V.; Finn, M.G.; Click chemistry in materials synthesis. 1. Adhesive polymers from copper-catalyzed azide-alkyne cycloaddition. *J. Polym. Sci. A Polym. Chem.* **2004**, 42 (17), 4392-4403.

13. Hafner, S.; Hardegen, V. A.; Hofmayer, M. S.; Klapötke, T. M.; Potential energetic plasticizers on the basis of 2,2-Dinitropropane-1,3-diol and 2,2-Bis(azidomethyl)propane-1,3-diol. *Propellants, Explos., Pyrotech*. **2016**, 41, 806-813.

14. Bellan, A, B.; Hafner, S.; Hartgenen, V. A.; Klapötke, T.M.; Polyurethanes based on 2,2-Dinitropropane-1,3-diol and 2,2-Bis(azidomethyl)propane-1,3-diol as potential energetic binders. *J. Appl. Polym. Sci.*, **2016**, 133, 43991-44000.

15. Klapötke, T. M.; Krumm, B.; Rest, S. F.; Suceska, M.; Polynitro containing energetic materials based on carbonyldiisocyanate and 2,2-Dinitropropane-1,3-diol. *Z. Anorg. Allg. Chem.* **2014**, 640 (1), 84-92.

16. Hiskey, M. A.; Naud, D. L.; Improved synthetic routes to polynitroheterocycles. *J. Energ. Mater*. **1999**, 17(4), 379-391.

17. Backus, J.K. Rigid Polurethane Foams. In *Handbook of Polymeric Foams and Foam Technology*; Klempner, D; Frisch, K.C.; Hanser, Munich, 1991; p 79.

18. Niyogi, S.; Sarkar, S.; Adhikari, B.; Catalytic activity of DBTDL in polyurethane formation. *Indian J. Chem. Technol.* **2002,** 9, 330-333.

19. Burgess, A.E.; Davidson, J.C.; "Kinetics of the Rapid Reaction between Iodine and Ascorbic Acid in Aqueous Solution using UV-Visible Absorbance and Titration by and Iodine Clock" *J. Chem. Educ.* **2014**, 91 (2), 300-304.